



Role of the mid-Holocene environmental transition in the decline of late Neolithic cultures in the deserts of NE China



Licheng Guo ^{a, b, c, *}, Shangfa Xiong ^{a, b, c, **}, Zhongli Ding ^{a, b, c}, Guiyun Jin ^d, Jiabin Wu ^{a, b, c}, Wei Ye ^e

^a Key Laboratory of Cenozoic Geology and Environment, Institute of Geology and Geophysics, Chinese Academy of Sciences, Beijing, 100029, China

^b University of Chinese Academy of Sciences, Beijing, 100049, China

^c Institute of Earth Sciences, Chinese Academy of Sciences, Beijing, 100029, China

^d Department of Archaeology, Institute of Cultural Heritage, Shandong University, Jinan, 250100, China

^e College of Geography and Environmental Sciences, Zhejiang Normal University, Jinhua, 321004, China

ARTICLE INFO

Article history:

Received 27 January 2018

Received in revised form

28 March 2018

Accepted 20 April 2018

ABSTRACT

The mid-Holocene environmental transition was characterised by global cooling and the abrupt weakening of the Northern Hemisphere monsoon systems. It is generally considered the key driver of the collapse of several mid-Holocene agricultural societies, on a global scale. However, only a few previous studies have tried to verify the climatic origin of the collapse of these societies, using the compilation of spatiotemporal data at a large scale. Especially, the nature of mid-Holocene human-environment interactions in the climatically-sensitive margin of the East Asian summer monsoon front remains to be thoroughly understood. However, a systematic compilation of archaeological data at a regional scale can be used to verify the role the mid-Holocene environmental transition played in the collapse of late Neolithic cultures in China. Here, we present a regional compilation of Holocene records from sub-aerial sedimentary deposits, lake sediments, and archaeological sites in the deserts of NE China and the adjacent regions to explore human-environment interactions during the mid-Holocene. Comparison of the records of Holocene climate change with the evolution of archaeological sites reveals that the mid-Holocene environmental transition resulted in ecosystem degradation in the deserts of NE China, rendering these areas much less habitable. Faced with substantially increased environmental pressures, the late Neolithic inhabitants used several subsistence strategies to adapt to the environmental transition, including change in agricultural practices and ultimately migration. Overall, our results support the view that a widespread mid-Holocene drought destroyed the rain-fed agricultural and/or plant-based subsistence economies, ultimately contributing to the collapse of late Neolithic cultures in NE China.

© 2018 Elsevier Ltd. All rights reserved.

Keywords:
Mid-Holocene environmental transition
Archaeological sites
Neolithic cultures
Monsoon
Desert
China

1. Introduction

The global climate during the current Holocene interglacial is usually considered to be substantially warmer than that of the Younger Dryas event (Dansgaard et al., 1989). Moreover, it has provided a relatively stable environmental context for the growth and development of human society. However, when thresholds of

the Earth system were crossed (Alley et al., 2003), abrupt and widespread climate changes with major impacts on social-ecological systems occurred repeatedly during the Holocene (Weiss et al., 1993; O'Brien et al., 1995; Alley et al., 1997; Cullen et al., 2000; deMenocal et al., 2000a; Thompson et al., 2002; Morrill et al., 2003; Staubwasser et al., 2003; Marchant and Hooghiemstra, 2004; Mayewski et al., 2004; Alley and Ágústsdóttir, 2005; Booth et al., 2005; Drysdale et al., 2006; Wanner et al., 2008, 2011; Moros et al., 2009; Zhao et al., 2009; Macdonald, 2011; de Boer et al., 2014; Sarkar et al., 2015; Shanahan et al., 2015; Solomina et al., 2015; Lillios et al., 2016; Saraswat et al., 2016). In addition, severe climatic deterioration has often been regarded as the determining factor leading to the collapse of several ancient agriculturally-based civilizations (Hsu, 1998; Weiss and

* Corresponding author. Institute of Geology and Geophysics, Chinese Academy of Sciences, 19 Bei Tu Cheng Xi Lu, Chaoyang District, Beijing, 100029, China.

** Corresponding author. Institute of Geology and Geophysics, Chinese Academy of Sciences, 19 Bei Tu Cheng Xi Lu, Chaoyang District, Beijing, 100029, China.

E-mail addresses: guoliccheng05@mail.igcas.ac.cn (L. Guo), xiongsf@mail.igcas.ac.cn (S. Xiong).

Bradley, 2001). Clearly, detailed spatiotemporal information concerning abrupt and widespread climate change is important for improving our understanding of climate forcing and human responses during the Holocene, and for appraising the possible consequences of extreme climate events under a global warming scenario.

The mid-Holocene environmental transition has attracted much attention from climate scientists and archaeologists, especially Holocene event 3 (HE3, ~4.2 ka), as termed by Bond et al. (1997), because it marks the termination of the Holocene climatic optimum (Perry and Hsu, 2000) and the initiation of the Neoglacial (Solomina et al., 2015). Existing records reveal that ocean surface temperatures decreased by ~1–2 °C during HE3 (Bond et al., 1997; deMenocal et al., 2000b), which persisted for ~300–600 years (Cullen et al., 2000; Perry and Hsu, 2000); while a total duration of up to ~1500 years was recorded in the North Atlantic (Bond et al., 1997, 2001). In addition, HE3 was punctuated by a series of geologically-rapid global cooling and/or dry events (Morrill et al., 2003; Marchant and Hooghiemstra, 2004; Booth et al., 2005; Shanahan et al., 2015) which were superimposed on the gradual drying trend of the mid-Holocene (Morrill et al., 2003; Mayewski et al., 2004; Wanner et al., 2008, 2011; Roberts et al., 2011). Associated with HE3 were the collapse of cultures in Pakistan (Staubwasser et al., 2003; Madella and Fuller, 2006; Macdonald, 2011; Giosan et al., 2012; Ponton et al., 2012; Leipe et al., 2014; Menzel et al., 2014; Prasad et al., 2014a), Mesopotamia (Weiss et al., 1993; Cullen et al., 2000; deMenocal, 2001), China (Jin and Liu, 2002; Wu and Liu, 2004; An et al., 2005; Innes et al., 2014; Zeng et al., 2016; Zhu et al., 2017) and Egypt (Thompson et al., 2002; Marshall et al., 2011; Phillipps et al., 2012).

In high latitudes of the Northern Hemisphere, a peak in detrital carbonate flux on the East Greenland Shelf at 4.7 ka signaled both the beginning of the Neoglacial and a southward expansion of the Arctic sea ice (Jennings et al., 2002). In Europe, a 4.2 ka drought event is recorded by multi-proxy data from a cave flowstone in Italy (Drysdale et al., 2006); diatom assemblages from Montcortès Lake in the Iberian Peninsula indicate that lake levels were lower during a pronounced dry interval from 2360 to 1850 BCE (Scussolini et al., 2011); a decrease in deciduous *Quercus* and *Pinus pinea*-type percentages in Southwest Iberia at ~4.2 ka suggests an abrupt shift to dry conditions (Lillios et al., 2016); and a synthesis of records from the Mediterranean reveals an unusually dry interval from 4.5 to 3.9 ka (Mercuri et al., 2011; Roberts et al., 2011). Evidence from eastern tropical Africa indicates a shift to drier conditions at ~4.0 ka (Marchant and Hooghiemstra, 2004), although at this time wetter conditions were maintained in West Africa (Russell et al., 2003) and in parts of South America (Marchant and Hooghiemstra, 2004); and magnetic and geochemical data from the Holocene sediments of Lake Tana in northwest Ethiopia confirm that the driest interval occurred at ~4.2 ka (Marshall et al., 2011), which is also identified in the Mount Kilimanjaro ice core (Thompson et al., 2002) and in the Mauritian lowlands (de Boer et al., 2014). In eastern Russia, evidence of a cold spell between 4.5 ka and 3.5 ka is provided by a multi-proxy record from Two-Yurts Lake (Hoff et al., 2015). A severe centennial-scale megadrought in mid-continental North America occurred between 4.1 and 4.3 ka (Booth et al., 2005).

In Asia, a record of the concentration of eolian minerals in core M5-422 from the Gulf of Oman reveals an abrupt increase in the content of eolian dolomite and CaCO₃ at ~4.1 ka, indicating the onset of dry conditions in Mesopotamia (Cullen et al., 2000); a planktonic oxygen isotope record from core 63 KA from the Arabian Sea shows a shift to heavier δ¹⁸O values at ~4.2 ka, indicating dry conditions in the Indus valley (Staubwasser et al., 2003); multiple lines of evidence from Lonar Lake indicate that the driest conditions in central India occurred from 4.8 to 4.0 ka (Prasad et al., 2014b;

Sarkar et al., 2015), in agreement with records from Wadhwana Lake of very dry conditions at ~4.3 ka, (Prasad et al., 2014a); a Holocene pollen record from the northwestern Himalayan lake Tso Moriri suggests that the prolonged Holocene trend towards aridity was punctuated by an interval of increased dryness between ~4.5 ka and 4.3 ka (Leipe et al., 2014); after ~5 ka, the forest vegetation in the Mongolian Altai began to give way to a predominance of open vegetation types as the precipitation amount decreased from 450 to 550 mm/yr to 250–300 mm/yr (Rudaya et al., 2009); the stable oxygen isotopic composition of authigenic lacustrine calcite from Xingyun Lake, in Yunnan Province in China, recorded a substantial positive shift from 5.0 to 4.3 ka, which is coincident with aridity in India and the Tibetan Plateau (Hillman et al., 2017); vegetation history during the Baodun period (~4.5–3.7 ka) in the Chengdu Plain reveals that the dry and cool climate conditions occurred at this period (Zeng et al., 2016); an abrupt climatic transition from wet to dry conditions at ~4.1 ka in the western part of the Chinese Loess Plateau (An et al., 2005), and an exceptional cold event at 4.6–4.3 ka in Hebei Province (Jin and Liu, 2002), indicate short-duration cold and dry events during the mid-Holocene in northern China; at ~4.2 ka there was an increase in cold-tolerant trees at Taihu Lake in the Yangtze coastal plain (Innes et al., 2014) and the climate in the middle reaches of the Yangtze River became rather dry and cold (Zhu et al., 2017); and a rapid and catastrophic fall of the groundwater table of up to ~30 m in the Otindag Desert at ~4.2 ka marks the onset of irreversible desertification in northern China (Yang et al., 2015).

Furthermore, several comprehensive reviews at a regional or global scale of Holocene glacier fluctuations (Solomina et al., 2015) and Holocene climate changes (An et al., 2006; Wanner et al., 2008, 2011; Rudaya et al., 2009; Zhao et al., 2009; Zhao and Yu, 2012; Wang and Feng, 2013) suggest that various climatic proxies recorded a cool and/or dry event in middle to low latitudes of Eurasia at ~5–4 ka. In addition, the wet status during this interval was confirmed in high latitudes of Eurasia (e.g., northern Xinjiang, the northern Mongolian Plateau, the Lake Baikal region and western Russia) as evaporation decreased (Rudaya et al., 2009).

Collectively, these cool and/or dry events in monsoon-influenced regions demonstrate that from 5 to 4 ka a significant large-scale drought in middle to low latitudes of the Northern Hemisphere was a primary response to an interval of weak monsoon strength. The consensus indicates that the mid-Holocene weak monsoon likely resulted from interacting ocean-atmosphere processes in the western tropical Pacific and the equatorial Indian Ocean, such as the El Niño Southern Oscillation (ENSO) (Moy et al., 2002; Marchant and Hooghiemstra, 2004; Macdonald, 2011) and the Indian Ocean Dipole events (Abram et al., 2007; de Boer et al., 2014); and from the southward migration of the Intertropical Convergence Zone (ITCZ, Haug et al., 2001; Wanner et al., 2008; Abram et al., 2009; Sarkar et al., 2015; Shanahan et al., 2015) or cold climatic conditions at high latitudes of the Northern Hemisphere (Bond et al., 1997; Menzel et al., 2014; Fan et al., 2016). In addition, a regional interpretation considered this to be an irreversible region-wide hydrologic event (Yang et al., 2015). Ecosystem degradation was one of the most important effects of HE3, resulting in the abandonment of dwellings and the migration of Neolithic peoples to more habitable areas (Hsu, 1998; Perry and Hsu, 2000; Giosan et al., 2012; Jia et al., 2016), and the forced modification of agricultural systems such as the increased cultivation of drought-tolerant crops like millet (Giosan et al., 2012) and the spread of wheat in East Asia (Dodson et al., 2013; Chen et al., 2015a). Giosan et al. (2012) suggested that the effects of HE3 caused a decrease in the total settled area and in settlement sizes in the Indus Valley since 3.9 ka. In addition, the combination of decreased agricultural productivity and increased population in habitable areas triggered

regional warfare during HE3, contributing to the decline and demise of several agriculturally-based civilizations.

Previous studies have used well-dated and high-resolution climatic sequences to decipher the relationship between late Neolithic cultural collapse and the mid-Holocene environmental transition. Several researchers argue that previous studies directly link the effects of the mid-Holocene environmental transition by one or multiple sequences to the late Neolithic cultural collapse. However, only a few studies have tried to verify comprehensively the mid-Holocene climatically-forced nature of the cultural collapses, using the compilation of spatiotemporal data at a large scale (An et al., 2005; Leipe et al., 2014; Lillios et al., 2016; Jia et al., 2017). Consequently, further work is needed to fully understand and explore how the mid-Holocene environmental transition affected civilizations in sensitive ecological environments, such as the desert-grassland border in the deserts of NE China. A compilation of archaeological data at a regional scale can be used to verify some of the hypotheses concerning past human-environment interactions in ecologically fragile environments (Hosner et al., 2016). For example, An et al. (2005) demonstrated that a decrease in the number of archaeological sites at ~4.0 ka in the western part of the Chinese Loess Plateau was a direct response to widespread aridification, with a shift from settled, rain-fed agriculture to migratory pastoralism. However, this work emphasized the cultural response within a small area, and it did not consider archaeological signatures at a large scale, such as those associated with, for example, long-term migration. Clearly, more work is needed which undertakes a large-scale compilation of archaeological data. The present research seeks to investigate human-environment interactions in the deserts of NE China during the mid-Holocene, using a regional compilation of Holocene records from sub-aerial sedimentary deposits, lake sediments, and archaeological sites in these deserts and the adjacent regions.

2. Regional setting

The deserts of NE China are in the northern margin of the region of influence of the East Asian summer monsoon (EASM); from east to west they are the Hulun Buir, Horqin, Otindag, Hobq and Mu Us deserts (Fig. 1). They are quite different from the large deserts situated to the west of the north-south-oriented Helan Mountains (~106°E), because the current climate of these deserts is semi-arid, dominated by a wet, warm EASM and a dry, cold East Asian winter monsoon (EAWM, Fig. 1). The annual precipitation of the entire area of these deserts decreases from 400 to 500 mm in the southeast to 200 mm in the northwest (Ren et al., 1985). EASM precipitation, from June to September, contributes as much as 65–75% to total annual precipitation (Liu, 2010). The natural vegetation of these deserts is temperate steppe (Ren et al., 1985), with for example Needlegrass (*Stipa* sp.) and Chinese wild rye (*Aneurolepidium chinense*). As an agro-pastoralism transitional zone, these deserts are a crucial area of cultural interaction and dispersal. In addition, several rivers flow through them, including the Yellow River and the Xilamulun, Xilaohe and Hailar Rivers, which support irrigation agriculture which enabled the region to be one of the cradles of ancient Chinese civilization (Liu and Chen, 2012).

3. Material and methods

3.1. Holocene dated records from sub-aerial sedimentary deposits in the deserts of NE China

EASM precipitation has a major effect on the vegetation distribution and dune activity in the deserts of NE China (Yang et al.,

2011). Abundant EASM precipitation favors plant growth and the development of paleosols and lakes, while a deficit of EASM precipitation results in dune reactivation; moreover, reactivated dunes are the major source of loess deposits in the margin of the deserts of NE China. Thus, paleosols and lacustrine and peat deposits (which are the sources of dated records of environmental stability in this research) are characteristic of intervals of relatively warm and wet climate; and conversely, associated with eolian sand and loess (the source of dated records for a sediment accumulation state) are a dry and cold climate, mainly due to the increased aridity resulting from reduced EASM precipitation and/or effective moisture (Lu et al., 2005; Mason et al., 2009). Furthermore, during the last two decades, paleoenvironmental and palaeoclimatic studies in these deserts have yielded a very large number of dated records indicating accumulation and environmental stability, corresponding to dune mobile and stable states, respectively (Lu et al., 2011, 2012).

It should be noted that (i) we selected published actual ages determined by radiocarbon or luminescence methods, (ii) used one dated record when multiple ages or similar ages were measured from the same layer at a site, and (iii) rejected ages that were not in stratigraphic order. This resulted in a total of 811 published dated records (329 dated records indicating dune mobile states and 482 dated records indicating dune stable states) from 268 sections (Fig. 1). Detailed information on these dated records is listed in Table 1. In addition, uncalibrated radiocarbon ages were calibrated to calendar years before present (BP) (BP = 1950 CE) using the Calib Rev 7.0.4 radiocarbon age calibration program (Stuiver and Reimer, 1993) with the IntCal13 curve (Reimer et al., 2013), prior to statistical analysis. The dated records are plotted as histograms with a bin width of 200 years, rather than with the Gaussian distribution approach (Singhvi et al., 2001) because in some areas there are intervals for which no dated records are available. The spatiotemporal distribution patterns of these dated records were illustrated using ArcGIS 10.2 with a Universal Transverse Mercator Projection coordinate system, based on the World Geodetic System 1984.

3.2. Holocene lake records from the deserts of NE China and adjacent regions

We compiled published records from 22 lake sections, including paleolake and peat sections, in the deserts of NE China and the adjacent regions (Fig. 1) to assess Holocene hydrological changes driven by variations in EASM precipitation. All the sections are listed in Table 2. A graphical synthesis of the data is used to illustrate the hydrological changes.

3.3. Archaeological data: sources and mapping

A total of 51,074 archaeological sites, ranging mainly from early Neolithic to early Iron Age, and covering most of the regions of China, has been published (Wagner et al., 2013; Hosner et al., 2016; <https://doi.pangaea.de/10.1594/PANGAEA.860072>). The resulting database increases our understanding of the evolution of Chinese civilization, especially changes in population, agricultural practices and subsistence strategies (Hosner et al., 2016). We used part of the database (30,519 archaeological sites) to establish the spatiotemporal distribution patterns of Holocene archaeological sites in the deserts of NE China and the adjacent regions using ArcGIS 10.2 with a Universal Transverse Mercator Projection coordinate system, based on the World Geodetic System 1984.

The ages of archaeological sites in each map, with a bin width of 1000 years, are constrained by ¹⁴C-dated cultural intervals and additional published data. Although the spatiotemporal

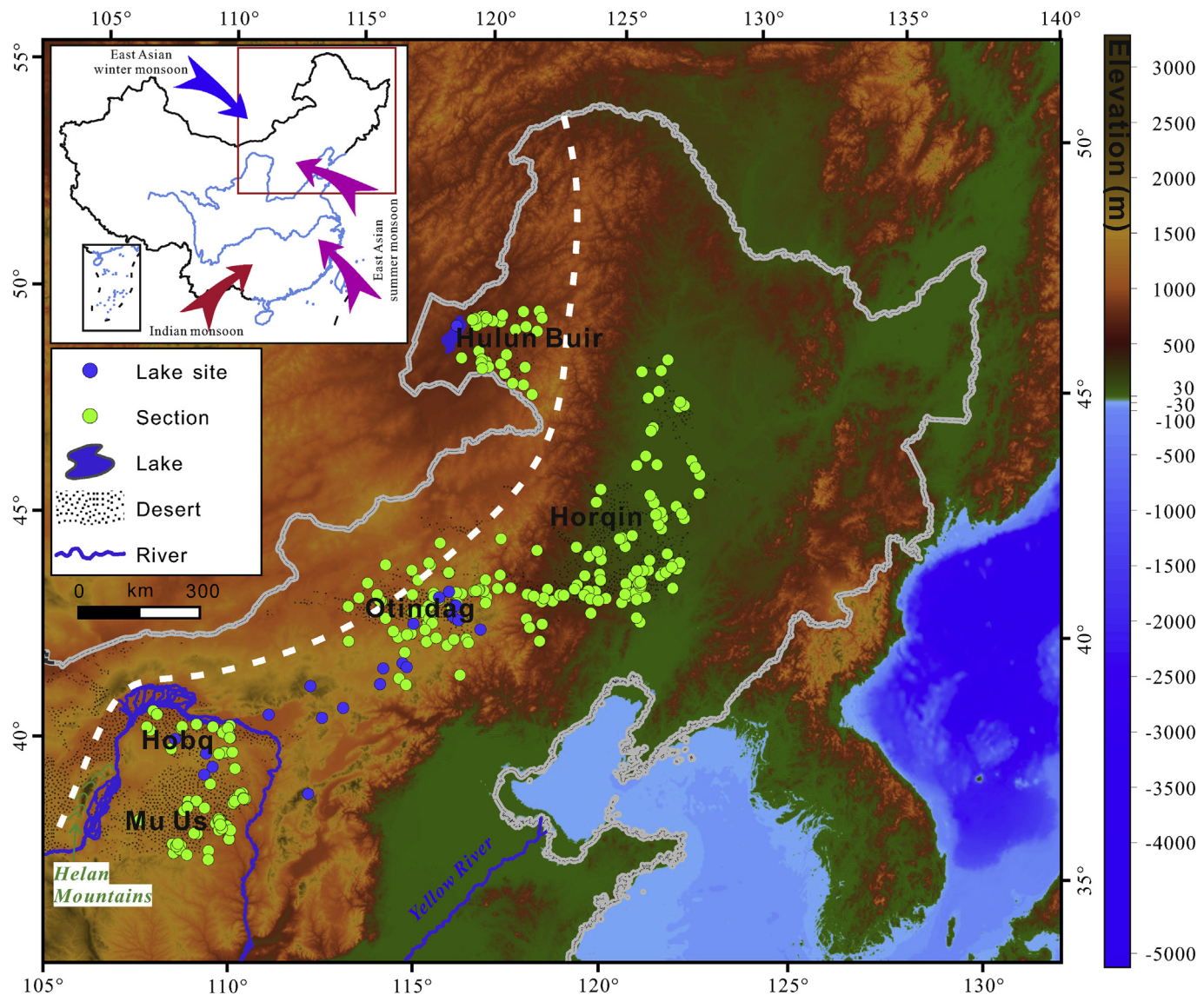


Fig. 1. Distribution of the deserts (Hulun Buir, Horqin, Otindag, Hobq and Mu Us) and study sites (sections and lake sites) in NE China along the margin of the East Asian summer monsoon front (white dashed line). This desert data set is provided by the Environmental and Ecological Science Data Center for West China, National Natural Science Foundation of China, <http://westdc.westgis.ac.cn>.

distribution patterns of Holocene archaeological sites have intrinsic disadvantages for depicting the evolution of ancient cultures (Ruddiman et al., 2008), they can verify the influence of the mid-Holocene environmental transition on the collapse of late Neolithic cultures in China (Hosner et al., 2016).

4. Results

4.1. Holocene dune activity in the deserts of NE China

The spatiotemporal distribution of states of dune stability and mobility in the deserts of NE China during the Holocene are shown in Figs. 2 and 3. For the five deserts, the numbers of dated records indicating dune mobile states exhibit relatively high values with a decreasing trend from ~12 to 9 ka; they then decrease for the interval of ~9–4 ka, with a minimum at ~4.5 ka, and gradually increase since ~4 ka. However, the numbers of dated records indicating dune stable states is lower, with an increasing trend from ~12 to 9 ka; they then increase rapidly and maintain relatively high

values during the interval from ~9 to 5 ka. From ~5 to 4 ka, a minimum in the number of stable state records is documented. Subsequently, since ~4 ka, the numbers of ages for stable states are relatively high and fluctuate with a large range. In addition, during

Table 1
Distribution of luminescence and radiocarbon ages from the deserts of NE China.

Region	Luminescence dates			Radiocarbon dates	Total	Number of sites
	OSL	IRSL	TL			
Hulun Buir	75	—	—	16	91	30
Horqin	204	—	2	87	293	107
Otindag	173	—	2	42	217	64
Hobq	28	—	—	7	35	16
Mu Us	97	2	6	70	175	51
Total	560	2	10	222	811	268

Note: ‘—’ indicates no data.

Abbreviations OSL, Optically Stimulated Luminescence; IRSL, Infrared-stimulated luminescence; TL, Thermoluminescence.

Table 2

Holocene lake and peat records from the deserts of NE China and the adjacent regions.

No.	Site	Latitude (°N)	Longitude (°E)	Elevation (m a.s.l.)	Archive	Present lake area(km ²)	Age range (cal. kyr BP)	Dating method	Number of dates	Proxy	Reference
1	Hulun Lake	49.127	117.506	545	Lake core	2339	11.1–0	AMS ¹⁴ C	14	GC, GS, OS, P	Xiao et al., 2009a; Wen et al., 2010; Zhai et al., 2011
2	Dali Lake	43.261	116.604	1226	Lake core	238	11.5–0	AMS ¹⁴ C	15	Ca, GC, GS, OM, P	Xiao et al., 2008, 2009b; Fan et al., 2016, 2017; Wen et al., 2017
3	Dali Lake	43.15	116.29	1226	Outcrop	238	16.0–0	OSL, AMS ¹⁴ C	41	Lithology	Goldsmith et al., 2017a, b
4	Haoluku	42.96	116.75	1295	Outcrop	dry	10.3–0	AMS ¹⁴ C	3	C/N, EM, GC, GS, LOI, OM, P	Wang et al., 2001; Liu et al., 2002
5	Haolaihure paleolake	42.951	116.794	1295	Outcrop	dry	12.2–0	AMS ¹⁴ C, OSL	13	C/N, D, GC, GS, OM	Guan et al., 2010; Liu et al., in press
6	Liuzhouwan	42.71	116.67	1365	Outcrop	dry	13.5–0	AMS ¹⁴ C	3	C/N, EM, GC, GS, LOI, OM, P	Wang et al., 2001
7	Xiaoniuchang	42.62	116.83	1460	Outcrop	dry	10.0–0	AMS ¹⁴ C	3	Ca, GC, P	Liu et al., 2002; Wang et al., 2004
8	Xiarinur Lake	42.6	115.47	1225	Lake	3.1	15.6–0	AMS ¹⁴ C, ²¹⁰ Pb/ ¹³⁷ Cs	17	EM, GS, P	Tang et al., 2015
9	Jiangjunpaozi	42.374	117.47	1490	Outcrop	dry	11.5–0	AMS ¹⁴ C	2	C/N, EM, GS, LOI, OM, P	Wang et al., 2004
10	Ulan Nuur	41.737	115.094	1246	Outcrop	<8.9	8.6–6.1	AMS ¹⁴ C	4	C/N, EM, OM, P	Wang et al., 2012a
11	Bayanchagan Lake	41.65	115.21	1355	Lake	15	12.5–0	AMS ¹⁴ C	9	P	Jiang et al., 2006
12	Bai Nuur	41.643	114.515	1346	Outcrop	<2.3	10.6–6.4	AMS ¹⁴ C	5	C/N, EM, OM, P	Wang et al., 2012a
13	Anguli Nuur	41.3	114.4	1315	Lake	47.6	10.9–0	AMS ¹⁴ C, ²¹⁰ Pb/ ¹³⁷ Cs	10	EM, GC, GS, OM, P	Liu et al., 2010; Wang et al., 2010; Yin et al., 2011
14	Diaojiao Lake	41.3	112.35	1800	Lake core	0.3	10.2–2.1	¹⁴ C	4	P	Shi and Song, 2003
15	Huangqihai Lake	40.8	113.3	1277	Outcrop	71.93	8.2–2.2	AMS ¹⁴ C, OSL	6	EM, GC	Shen et al., 2005, 2010; Chen et al., 2008
16	Chasuqi	40.67	111.12	1000	Outcrop	peat	9.1–0	¹⁴ C	4	P	Wang et al., 1999
17	Daihai Lake	40.586	112.668	1230	Lake core	133.5	12.3–0	AMS ¹⁴ C	8	Ca, GS, OM, P	Xiao et al., 2004, 2006; Peng et al., 2005; Xu et al., 2010; Chen et al., 2003
18	Yanhaizi Lake	40.1	108.4	1180	Lake core	<18	17.0–0	AMS ¹⁴ C	15	EM, GC, Lithology, OM	Jiang et al., 2014
19	Bojianghaiizi Lake	39.793	109.309	1365	Lake core	1.2	11.8–0	AMS ¹⁴ C	10	GS, LOI, P	Sun and Feng., 2013
20	Qigai Nuur	39.5	109.5	1403	Lake core	5	10.7–0	AMS ¹⁴ C	17	P	Feng et al., 2005; Guo et al., 2007;
21	Baahar Nuur	39.32	109.27	1278	Lake core	dry	11.9–0	AMS ¹⁴ C	15	Ca, EM, GC, GS, OM, P	Huang and Guo, 2017
22	Gonghai Lake	38.9	112.233	1860	Lake core	0.36	14.7–0	AMS ¹⁴ C, ²¹⁰ Pb/ ¹³⁷ Cs	25	Ca, EM, GC, GS, OM, P,	Chen et al., 2013, 2015b; Rao et al., 2016; Liu et al., 2018

Abbreviations Ca—Carbonate content, D—Diatoms, EM—Environmental magnetic proxies, GC—Geochemical proxies, GS—Grain size, OM—Organic matter content, OS—Ostracod assemblage, P—Pollen.

the late Holocene, there are few documented stable state records for the Mu Us desert, which likely results from local human activity involving over-grazing and over-cultivation. The synthesis of states of Holocene dune stability and mobility from the five deserts emphasizes several broad trends: a regional reversal of dune mobility and/or semi-stability (~12–9 ka) to dune stability and paleosol development (~9–5 ka); and sporadic dune re-mobilization beginning at ~5 ka, and dune re-mobilization throughout the entire study region since ~4 ka.

In addition, although Holocene dated records of sub-aerial sedimentary deposits should be documented in all the selected sections in the deserts of NE China, in practice, stratigraphic discontinuities in the various geomorphic units and limitations of the

sampling strategies somewhat limit the utility of the data set (Li and Yang, 2016). Thus, the maximum in the number of total dated records is treated as the upper limit of the number of dated records for each time slice in these deserts. Based on this approach, a new proxy, the activation ratio, was calculated, as follows: activation ratio = number of dated records/max [number of total dated records], and it can be used to evaluate the number of occurrences of a potentially reactivated state. The activation ratio has relatively high values from ~12 to 9 ka, lower values from ~9 to 4 ka, and increases gradually since ~4 ka. Comparison of the activation ratio with the spatiotemporal distribution of Holocene dune stable and mobile states in these deserts, leads to the conclusion is that the onset of widespread dune re-mobilization occurred at ~4 ka (Fig. 4).

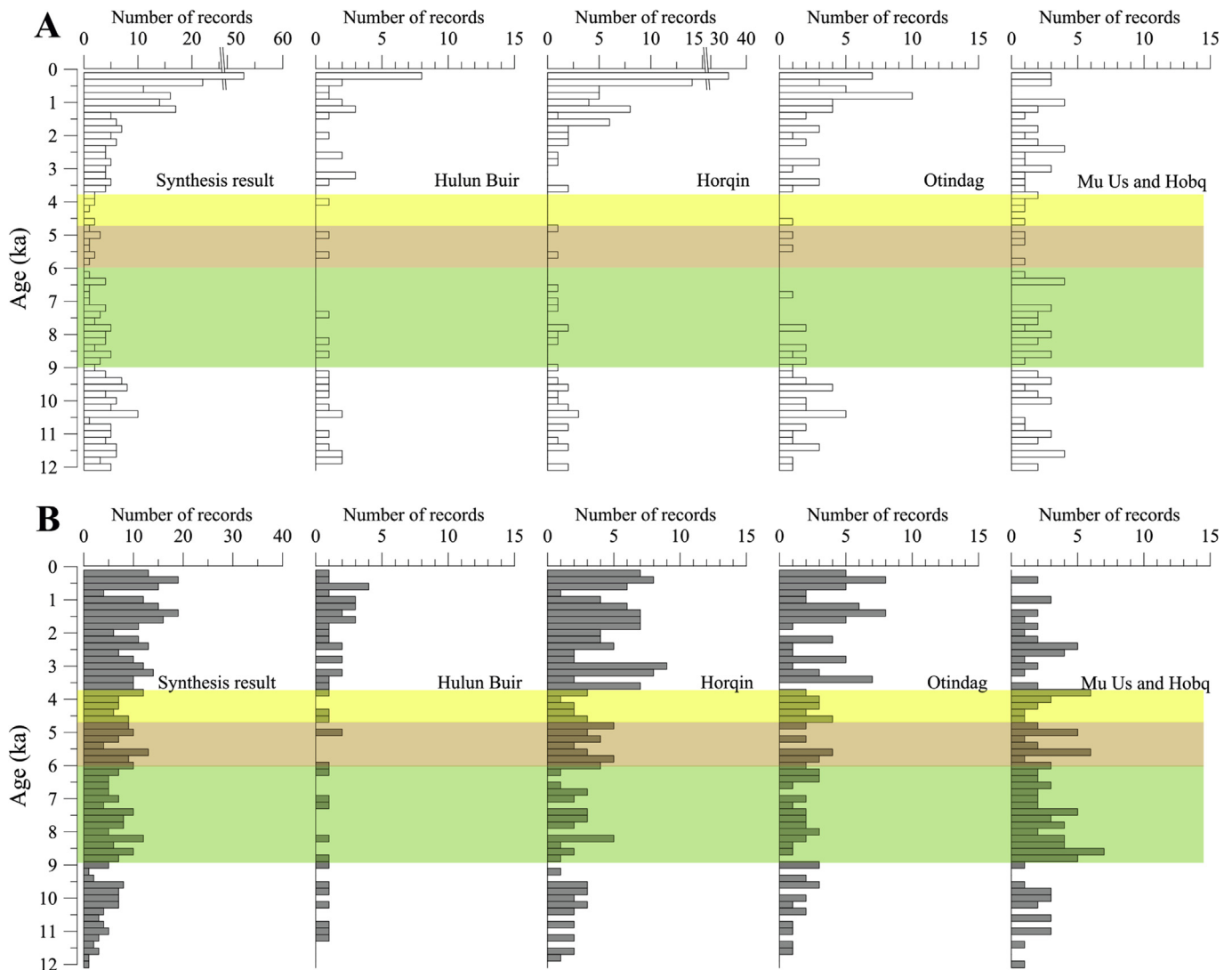


Fig. 2. Histogram of Holocene dated records for dune mobile (A) and stable (B) states in the deserts of NE China. The humid periods are shown by green rectangles and dry (driest) periods are shown by light orange (yellow) rectangles, respectively. (For interpretation of the references to color in this figure legend, the reader is referred to the Web version of this article.)

4.2. Holocene hydrological changes in the deserts of NE China and adjacent regions

The Holocene hydrological changes in the deserts of NE China and the adjacent regions are summarized in Fig. 5; the data comprise 22 lake records (Table 2). Analysis of climatically-sensitive proxies (e.g., pollen and ostracod assemblages, organic matter and carbonate content, grain size, and geochemical parameters) enables four shifts to be observed, at around 11, 9, 6, and 4.3 ka. A warmer and wetter climate at Daihai lake and a high lake level in Hulun and Dali lakes confirm that the timing of the wettest climate along the margin of the EASM front was from ~9 to 6 ka. However, during the interval from ~11 to 9 ka, Hulun and Dali lakes maintained a high stand, in response to inflowing water to both lakes which resulted from insolation-driven snow/ice melt from the surrounding mountains and/or groundwater (Wen et al., 2010, 2017). During the mid-Holocene, conditions became drier and lake shrinkage occurred, starting at ~6 ka; this was followed by a semiarid interval from ~6 to 4 ka. The other prominent feature of the data is that from ~4.3 ka the lakes in these deserts and the adjacent regions shifted entirely to a low lake level state in

response to an intensification of aridification. The shrinkage of the lakes continued towards the present. In addition, when the lake area is too small or the number of dates less is than 4, the lake records exhibit several asynchronous shifts (e.g., at Baahar Nuur, Jiangjunpaozi, Xiaoniuchang, and Liuzhouwan).

4.3. Spatiotemporal distribution of archaeological sites in NE China during the Holocene

Seven time-slices from the selected 30,519 archaeological sites in NE China are used to establish the spatiotemporal distribution patterns of archaeological sites in NE China during the Holocene (Fig. 6). They show a long-term trend of an increase in the number of archaeological sites in NE China. From ~7 to 5 ka, the number of archaeological sites in the deserts of NE China reached a maximum. Comparison of the late Neolithic (5–4 ka, Fig. 6) and early Bronze Age (4–3 ka, Fig. 6) time slices, reveals that the number of archaeological sites decreased in the deserts, but increased substantially in the middle to lower reaches of the Yellow River. In contrast to the late Neolithic time slice, a similar distribution pattern of archaeological sites in NE China occurred from ~3 to 2 ka,

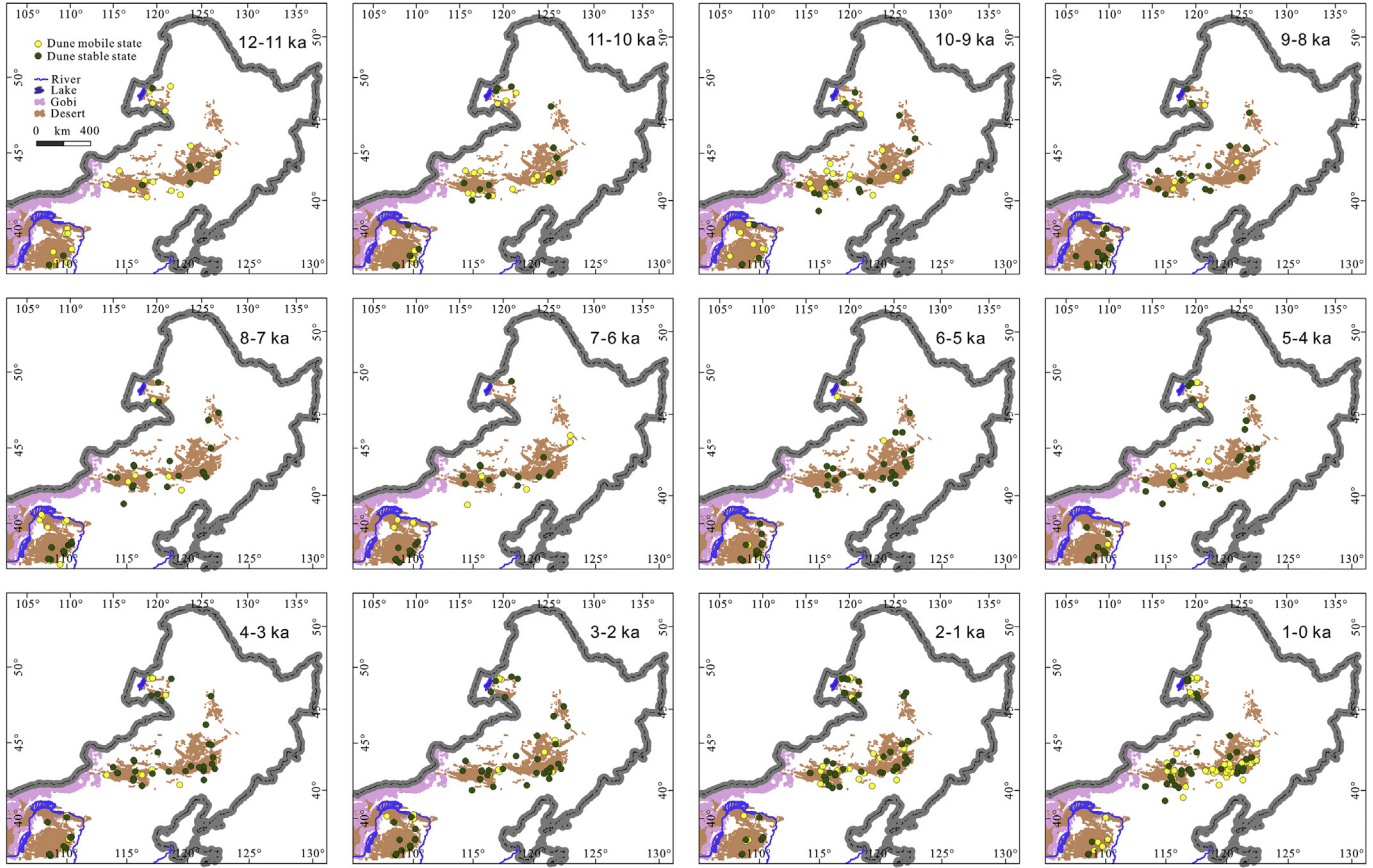


Fig. 3. Spatiotemporal distributions of Holocene dated records of sub-aerial sedimentary deposits in the deserts of NE China. These dated records for dune mobile and stable states indicate Holocene dune activity in these deserts. The extent of the deserts in all maps only reflects its modern status.

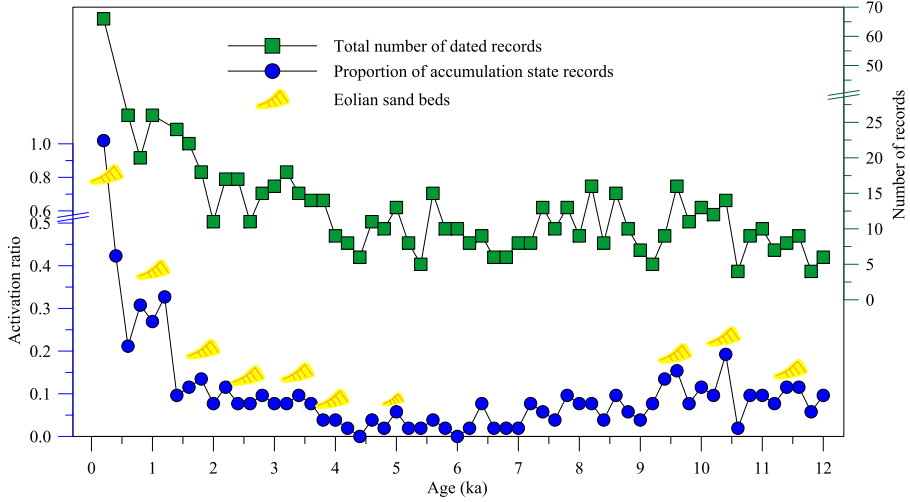


Fig. 4. Total number of dated records and activation ratio in the deserts of NE China over the last 12 kyr. The appearance of eolian sand bed is inferred from the dated records for dune mobile states (a low number indicates weak and/or sporadic dune re-mobilization). Activation ratio = number of dated records/max[number of total dated records].

with the difference resulting from a substantial increase in the number of archaeological sites in the North China Plain.

It is noteworthy that the age of each archaeological site was constrained by one dated interval; thus, we used the median age to confirm the time slice for each site. The dating half-intervals of the selected 30,519 archaeological sites in NE China are shown in Fig. 7; they are less than 600 years from ~5 to 4 ka, although there is a

large half-interval of up to 3000 years at ~7 ka. The large half-interval from ~7 to 5 ka (Fig. 7) also yields a data artifact in that the site distribution in NE China during the period of ~7–6 ka is much denser than during the subsequent period (~6–5 ka). In fact, the former period was when Zhaobaogou and probably the early Hongshan culture developed, while the latter period was when the Hongshan culture flourished, with site numbers multiplying from

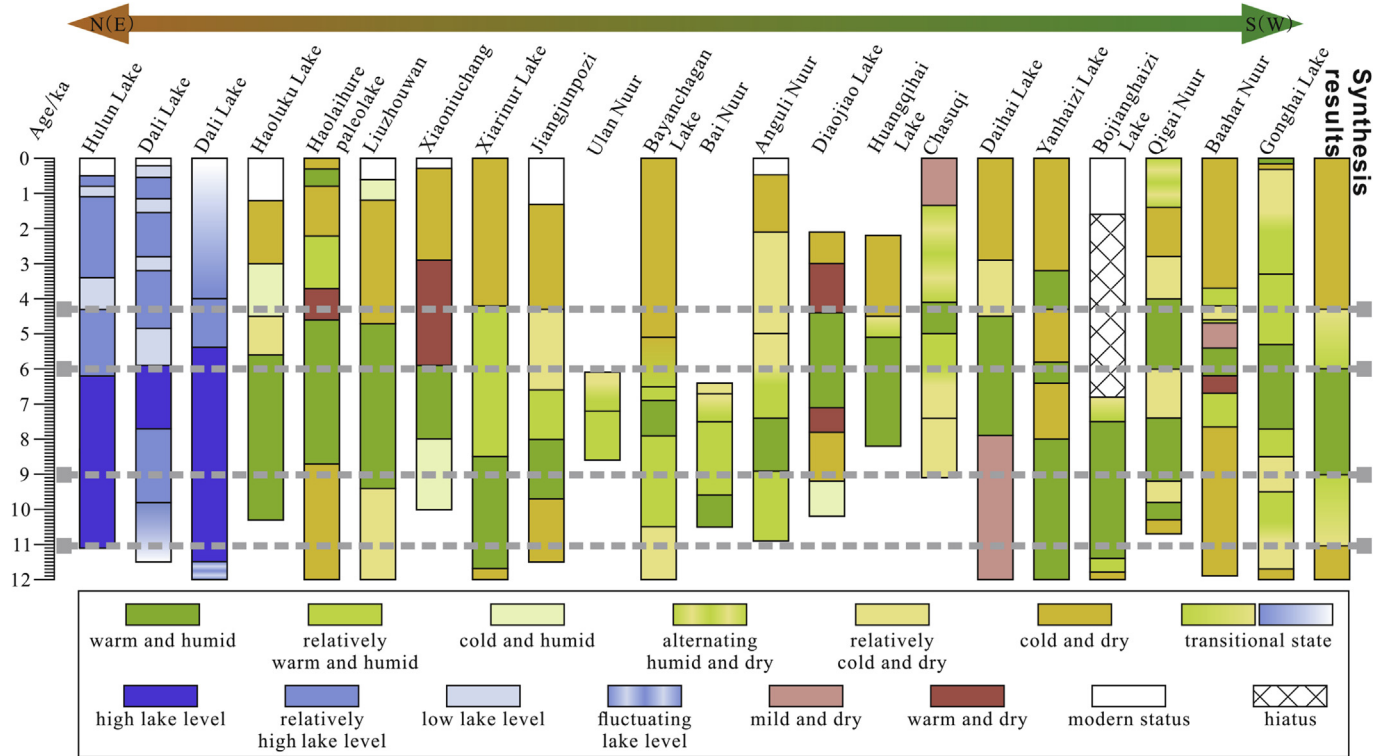


Fig. 5. Synthesis of Holocene hydrological changes of lakes in the deserts of NE China and the adjacent regions over the last 12 kyr (see Fig. 1 for site locations). Four shifts (11, 9, 6, and 4.3 ka.) were identified by analyzing climatically-sensitive proxies in these lakes.

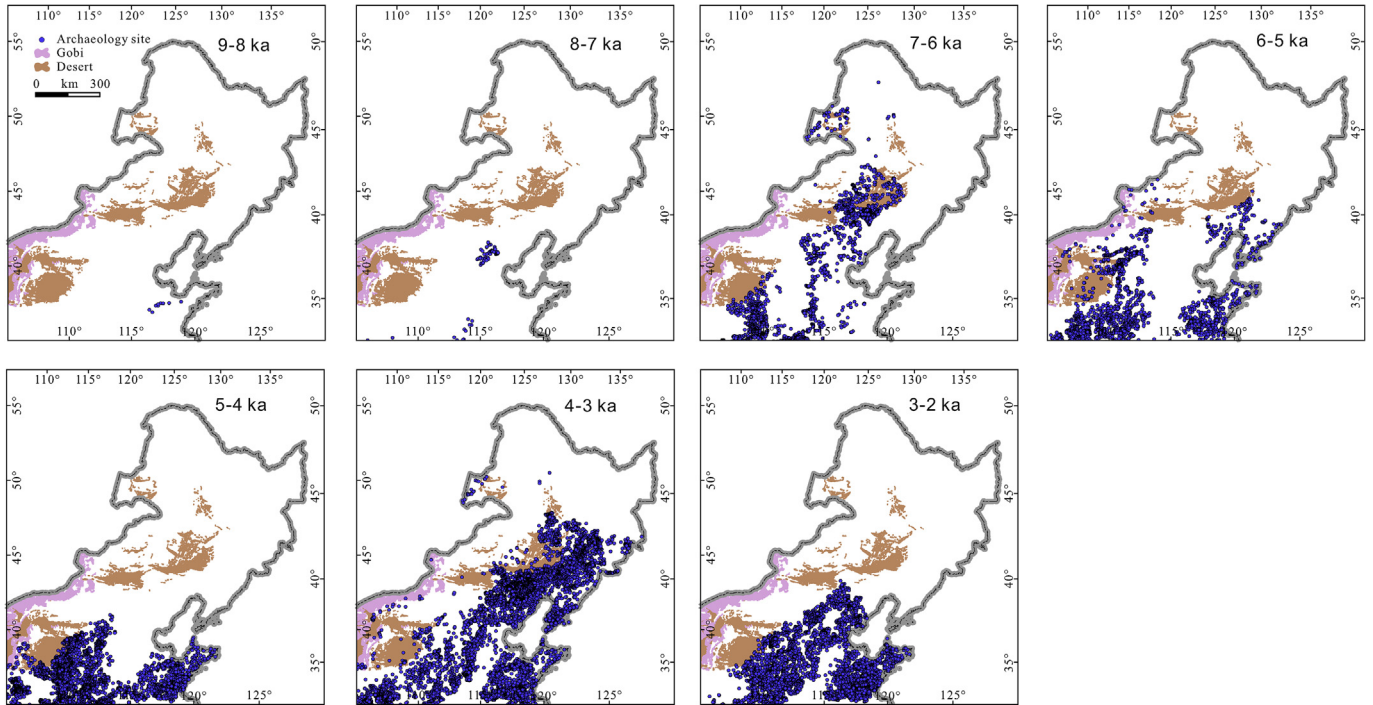


Fig. 6. Spatiotemporal distribution of archaeological sites in NE China during the Holocene. The archaeological sites are provided by Hosner et al. (2016) and can also be found in the open access PANGAEA Data Publisher for Earth & Environmental Science (<https://doi.pangaea.de/10.1594/PANGAEA.860072>). The extent of the deserts in all maps only reflects its modern status. The status of the deserts in different periods within the Holocene can be referred from the Holocene dune activity in the deserts of NE China (Fig. 4).

the previous period. Thus, the millennial-scale spatiotemporal distribution of archaeological sites in the deserts of NE China can be

confirmed during the mid-Holocene and we suggest that it confirms the impact of climate on prehistoric cultures of the late

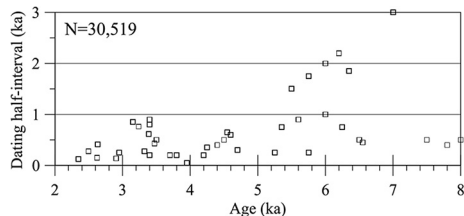


Fig. 7. Dating half-interval (shown in ka) of archaeological sites in NE China during the Holocene.

Neolithic – Bronze Age transition in the region.

5. Discussion

5.1. Mid-Holocene environmental transition in the deserts of NE China

Previously published multi-proxy records from along the margin of the EASM front directly and/or indirectly reveal that EASM precipitation increased gradually in the early Holocene (Peterse et al., 2011), reached a peak between 8 and 5 ka (Zhao and Yu, 2012; Lu et al., 2013; Wang and Feng, 2013; Guo et al., 2018), and that a striking mid-Holocene environmental transition with an abrupt shift to lower precipitation occurred at ~4 ka (An et al., 2006; Zhao and Yu, 2012). The pattern of Holocene environmental changes in the deserts of NE China indicated by our synthesis reveals a similar pattern. However, regarding mid-Holocene dune stabilization and mobilization in these deserts (Figs. 2 and 3), the dated records indicate a substantial decrease in dune stable states from ~5 to 4 ka, as well as in dune mobile states during ~6–4 ka, while the number of dated records for dune mobile states increases after ~4 ka. In addition, the lakes records show that the status of lakes in the deserts of NE China deteriorated gradually during the interval from ~6 to 4 ka, with lowest levels and hence driest conditions at ~4.3 ka (Fig. 5). These characteristics suggest that large-scale environmental deterioration in these deserts began from ~6 ka, and that dune re-mobilization throughout the entire area commenced at ~4 ka.

Our conclusions are supported by several syntheses using similar dated records of sedimentary deposits in other regions. The frequency distribution of the ages of loess and palaeosol layers on the Chinese Loess Plateau (Fig. 8b, Wang et al., 2014a) indicates a rapid decrease in the development of paleosols at ~6 ka, with a relatively low probability density of paleosols during the interval from ~6 to 4 ka. In addition, the accumulation rate of loess increased rapidly at ~5 ka, which was followed by a low probability density at ~5–4 ka. An early synthesis of results from the deserts of northern China and the Sahara based on humidity indicators (Fig. 8c, Guo et al., 2000) indicated that a series of dry events began at ~6 ka. Thus, a predominant characteristic of the Holocene history of the deserts of NE China is that the climate was semiarid from ~6 to 5 ka and subsequently became very cold and dry during the interval from ~5 to 4 ka. This cold and dry interval likely corresponded to HE3 which was a worldwide phenomenon, as noted in the introduction.

The abrupt weakening of the insolation-driven strength of the EASM is considered the cause of the mid-Holocene environmental transition in the deserts of NE China and the adjacent regions (Xiao et al., 2009a; Yang et al., 2013; Fan et al., 2016), in response to decreased Northern Hemisphere summer insolation at ~5 ka (Fig. 8d, Laskar et al., 2004). Decreased Northern Hemisphere summer insolation forced the southward migration of the ITCZ (Haug et al., 2001), reflected by increased percentages of ice rafted

debris in the North Atlantic (Fig. 8e, Bond et al., 1997), which weakened the EASM intensity. Simultaneously, due to decreased Northern Hemisphere summer insolation, sea surface temperatures of the western tropical Pacific decreased (Fig. 8f, Stott et al., 2004). Low latitude ocean-atmosphere thermodynamical effects likely induced an El Niño-like state (Fig. 8g, Moy et al., 2002) and ultimately weakened the EASM intensity. A weakened EASM could not transport sufficient water vapor from oceanic sources, which decreased EASM precipitation along the margin of the EASM front.

An et al. (2006), Zhao and Yu (2012) and Wang and Feng (2013) summarized the pattern of Holocene climate change on the margin of the EASM front, mainly focusing on moisture evolution reconstructed from pollen-based proxies. Their reviews indicate that the termination of peak moisture conditions in these deserts was from ~5 to 4 ka, which suggests a lag of ~1–2 kyr compared with our own conclusions. The pollen-based proxies are underpinned by the fact that effective moisture limits the growth and distribution of plants (Mason et al., 2009; Lu et al., 2011). When the Northern Hemisphere summer insolation decreased during the mid-Holocene, the temperature of the deserts of NE China decreased synchronously, which slightly altered effective moisture levels, but the thresholds of the ecological system were not crossed. Thus, tree pollen percentages and estimated C₄ biomass maintained relatively high values (Fig. 9) which was accompanied by dated records for dune stable states (Figs. 2 and 3) from ~6 to 5 ka, which explains the ~1–2 kyr lag observed in our data compared to that derived from pollen-based reconstructions.

5.2. Onset of dune re-mobilization in the deserts of NE China

The onset of dune re-mobilization in the deserts of NE China inferred from our results was at ~4 ka, in agreement with records from shoreline dunes from the Otindag Desert (Yang et al., 2015), coincident with a drastic decrease in EASM precipitation during the mid-Holocene. However, an important question is why dune re-mobilization throughout the entire study region did not begin at ~5 ka, because our conclusion suggests that the climate was rather cold and dry during the interval from ~5 to 4 ka, and even that the onset of dry conditions occurred at ~6 ka.

Several factors affect the development of dunes that reflect the onset of dune re-mobilization, including sand source, wind, landforms and local climate. The deserts of NE China are in endorheic basins which are well-supplied with sand derived from fluvial and alluvial sediments brought by rivers and streams from the surrounding mountains (Yang et al., 2012). Thus, climatic conditions in the sand source and depositional regions are often considered one of the limiting factors for the development of dunes in these deserts. Precipitation in sand source regions affects the development of fluvial and alluvial sediments and indirectly determines the supply of sand; and in depositional regions it influences the development of vegetation which is regarded as a major factor determining the sand transport rate (Liu et al., 2005).

During the interval from ~6 to 5 ka, the EAWM intensity decreased abruptly but still maintained a relatively high level (Fig. 8h, Wang et al., 2012b), with sparse vegetation cover in these deserts (Fig. 9), which prevented the dunes from expanding. Subsequently, the EAWM reached its weakest state during HE3 when the severe cold and dry conditions in the surrounding mountains resulted in insufficient sand supply for the development of dunes from ~4.2 ka. In contrast, at ~5 ka, the relatively stronger EAWM, with semiarid conditions in the surrounding mountains, was still able to supply sufficient sand to enable partial reactivation of those dunes which were not vegetation covered. Although vegetation covered part of these deserts after ~4 ka (Fig. 3), the thresholds of the ecological system were crossed, as indicated by the evidence

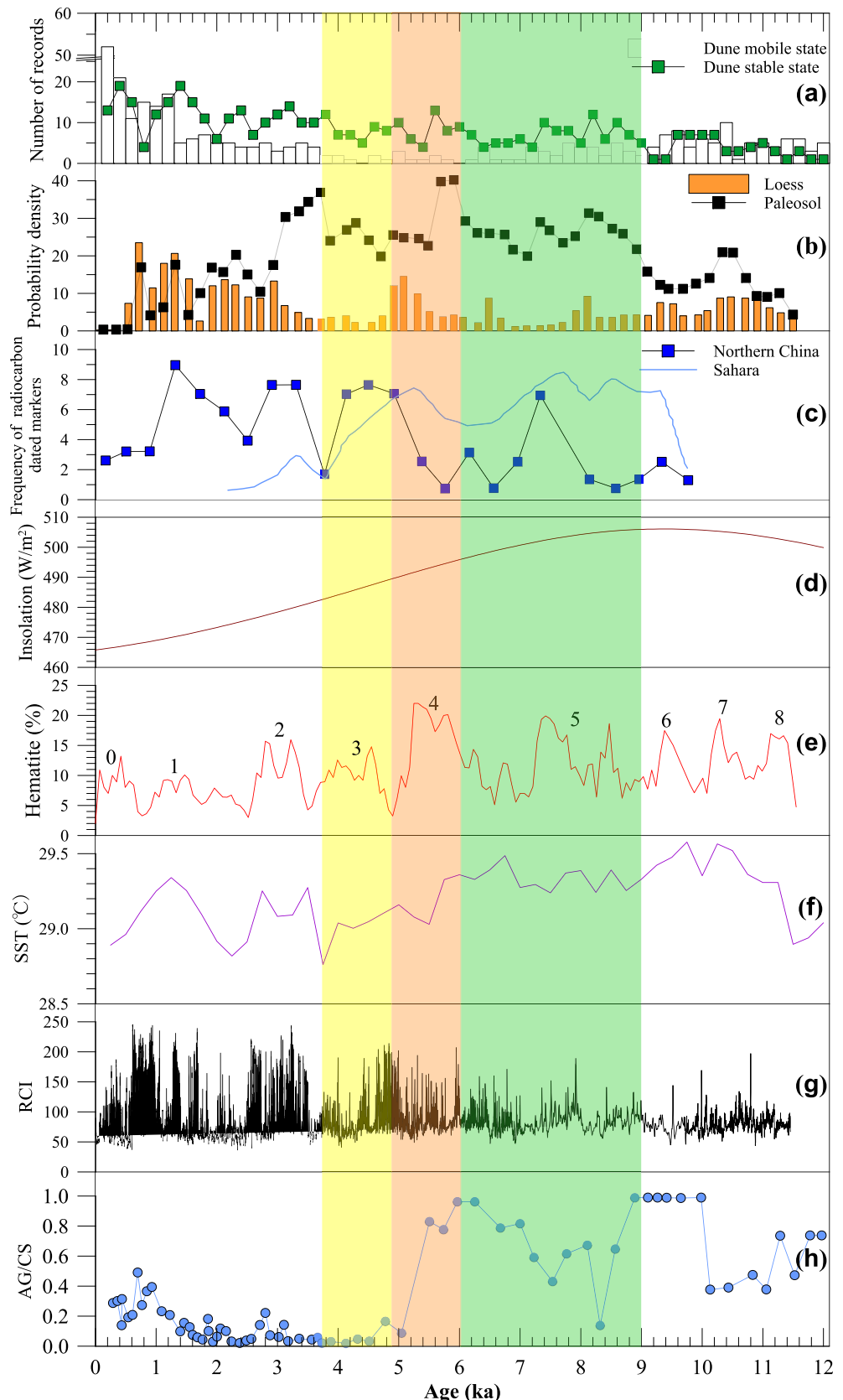


Fig. 8. Holocene dated records of sub-aerial sedimentary deposits (a, this study) in the deserts of NE China compared with the frequency distribution of Chinese Loess Plateau loess and palaeosol dates (b, Wang et al., 2014a); humidity indicators of deserts in northern China and the Sahara (c, Guo et al., 2000); July (China summer) insolation at 65°N (W/m^2) (d, Laskar et al., 2004); concentration of hematite-stained quartz grains in North Atlantic sediments (e, Bond et al., 2001) with 0–8 designating millennial-scale cycles; red colour intensity of a sediment core from Laguna Pallcacocha, southern Ecuador (g, Moy et al., 2002); sea surface temperature (SST) of the western tropical Pacific (f, Stott et al., 2004); and positive index for the strength of the EASM inferred from the AG/CS ratio, A. granulata/C. stelligera (h, Wang et al., 2012b). Rectangle colors are the same as in Fig. 2. (For interpretation of the references to color in this figure legend, the reader is referred to the Web version of this article.)

presented herein for severe cold and dry conditions from ~4.2 ka (Yang et al., 2015), which weakened the effect of vegetation on the sand transport rate. Thus after ~4 ka, the severe environmental conditions began to ameliorate slightly in the sand source regions with the gradual increase in EAWM intensity and/or human activities, which favored the development of dunes.

5.3. Effect of the mid-Holocene environmental transition on late Neolithic cultures in NE China

During the Holocene Thermal Optimum, warm and wet conditions along the margin of the EASM front favored the development of rain-fed agriculture in many flat and fertile terraces and alluvial fans, which provided a large area of arable land and a favorable habitat for Neolithic peoples. Thus, rain-fed agriculture played a major role in the flourishing of the Yangshao and Hongshan cultures (~5000–3000 BCE) in northern China (Crawford, 2009; Liu and Chen, 2012; Jia et al., 2017). The climate in northern China became slightly drier and cooler from ~6 to 5 ka, but this did not adversely affect the rain-fed agriculture of the Yangshao and Hongshan cultures. In addition, since the hydrothermal configuration in northern China meets the needs of rain-fed agriculture, the slightly drier and cooler climate stimulated the expansion and communication of the Yangshao and Hongshan cultures, which promoted the appearance of the short-lived culture in the Huang-qihai (Mo et al., 2003). In the case of the Yangshao culture, the size of settlements ranged from ~100 m² to more than 100 ha, the number of sites increased dramatically, and the distribution of sites expanded northwards to Inner Mongolia during this interval. The remains of domesticated plants (millet and rice) and animals (pigs and dogs) indicate that farming societies in central to southern Inner Mongolia were established (Ren and Wu, 1999). The quantity

of the bones of domestic pigs and dogs at Miaozigou site in the Huangqihai from ~3500 to 3000 BCE was 13% greater than in the same region at ~4500 BCE (Huang, 2003), and a possible interpretation of this is that the domesticated animals were fed on the abundant cereal crops (Zhang et al., 2010a). In addition, before 3500 BCE in central-south Inner Mongolia, subsistence strategies based on plants with various underground storage organs provided staple foods (Liu et al., 2016a). In contrast to the Yangshao culture, the Hongshan culture was the first complex society to develop in NE China, indicated by a dramatic increase in the number of sites and many new pottery types and a highly specialized type of jade work (Liu and Chen, 2012; Drennan et al., 2017). In addition, the earliest leaf-shaped and rectangular stone knives at Niuheliang site of the Hongshan culture likely were used to harvest cereal crops (Mo et al., 2003; Li, 2008), which demonstrates that the Hongshan people were cultivators. Evidence from paleodiet studies at several sites in the Liao River region of NE China reveal that during Hongshan culture, C₄-plant-based foods were primarily consumed for subsistence (Zhang et al., 2003; Liu et al., 2012). The main contribution of C₄-plant-based in the paleodiet is from millet agriculture (Zhao, 2004, 2011; Li, 2008). However, investigations of the functions of grinding stones recovered at Baiyinchanghan site of the Hongshan culture suggest that the people utilized a broad-spectrum subsistence strategy using various wild, cultivated, and domesticated plants (Liu et al., 2016b).

During the subsequent Laohushan (~2500–2300 BCE) and Xiaoheyan (~3000–2000 BCE) cultures in northern China (Liu and Chen, 2012), the EASM weakened and dunes began to be reactivated in the deserts of NE China. Thus, during the interval from ~5 to 4 ka, the mid-Holocene environmental transition undoubtedly would have led to the failure of rain-fed irrigation agriculture and thus to a conflict between decreased agricultural productivity and

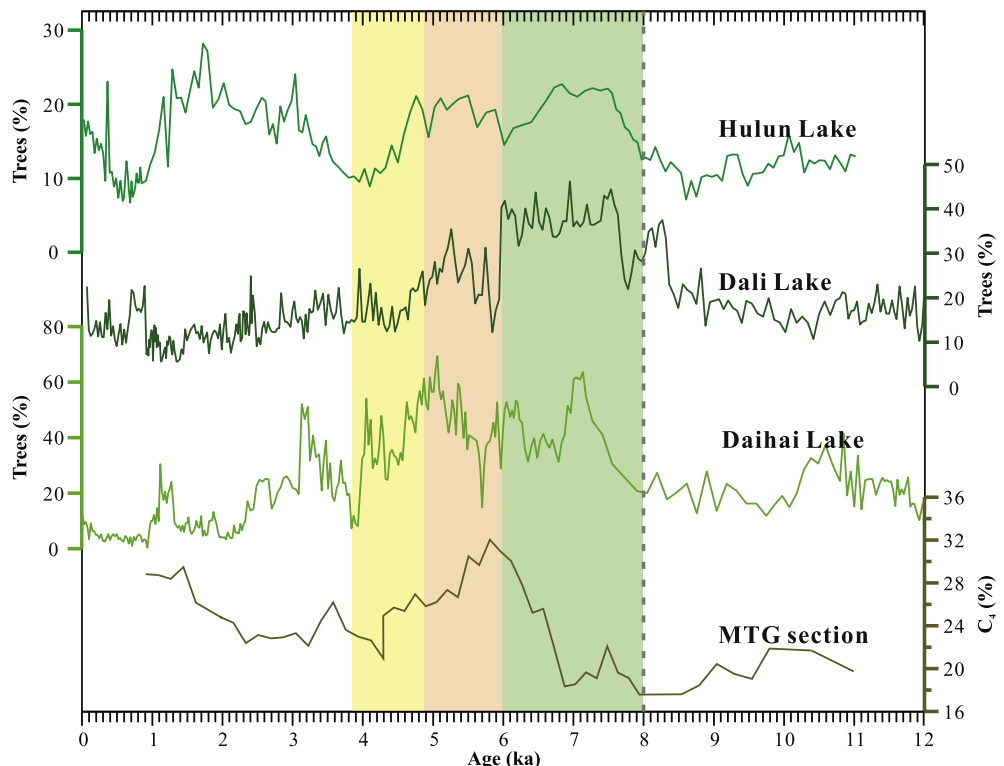


Fig. 9. Holocene vegetation records from estimated C₄ biomass of the MTG section in the Horqin Desert (Guo et al., 2018) and tree pollen percentages at Hulun Lake (Wen et al., 2010), Dali Lake (Wen et al., 2017) and Daihai Lake (Xiao et al., 2004) in the northern margin of the East Asian summer monsoon, in response to monsoon intensity changes. Rectangle colors are the same as in Fig. 2. (For interpretation of the references to color in this figure legend, the reader is referred to the Web version of this article.)

the increased population of previously habitable lands. Drier and cooler conditions in Inner Mongolia resulted in the disappearance of the short-lived culture in the Miaoziogou area and the ensuing cultural hiatus lasted some 1500 years (Mo et al., 2003). In addition, studies of past human-environment interactions in the Otindag Desert (Yang et al., 2015) and in the Taishizhuang section (Jin and Liu, 2002) reveal that a cold and dry event caused a reduction in the size of settlements, rapid abandonment of dwellings, and migration to the moister monsoon regions at ~4.2 ka. To adapt to the transition to the cold and dry environment of the mid-Holocene, frost-resistant wheat and/or barley likely were introduced to central-southern Inner Mongolia as the basis for subsistence during the late Neolithic period (Dodson et al., 2013; Liu et al., 2016a). In addition, the late Neolithic peoples on the eastern margin of the Mu Us Desert used vegetation to provide fuel for pottery manufacture, cooking and for heating (Miao et al., 2016). However, the development of the Hongshan culture in some regions relied mainly on millet cultivation (Zhang et al., 2003; Zhao, 2004, 2011; Li, 2008; Liu et al., 2012), and the cold and dry conditions during the subsequent Xiaoheyan culture impeded millet cultivation. Although the Neolithic peoples used a broad-spectrum subsistence strategy in central-southern Inner Mongolia and the Liao River region, such as the consumption of roots, tubers and nuts (Liu et al., 2016a, 2016b), the mid-Holocene environmental transition may have also affected the yields of oak and other nut-bearing trees as well as that of tuberiferous plants. Thus, the Xiaoheyan culture exhibited a lower level of social complexity with smaller populations, pastoralism, greater mobility of dwelling sites, abandonment of large ritual sites and limited jade-working (Li, 2008; Liu and Chen, 2012). Furthermore, several researchers have attributed the collapse of the Hongshan complex society to a large-scale drought event in northeast China (Jin, 2004; Li, 2008), where the summer monsoon rainfall reached a minimum at ~4.9 ka, as recorded at Lake Sihailongwan (Schettler et al., 2006).

Based on the regional compilation of records, a drastic decrease in the number of archaeological sites in the deserts of NE China during ~5–4 ka (Fig. 6) confirms that the mid-Holocene environmental transition resulted in ecosystem degradation (Jin and Liu, 2002; Tarasov et al., 2006), rendering land that was agriculturally productive during the Holocene Thermal Optimum subsequently unproductive, and reducing the overall habitability of the region.

Faced with the environmental severity, the late Neolithic farmers likely migrated from the deserts to the middle and lower reaches of the Yellow River or other habitable areas during ~5–4 ka. The reasons for these chosen destinations were that the middle and lower reaches of the Yellow River were warmer and moister and thus more favorable for habitation and farming compared with the northern deserts (Jin and Wang, 2010; Liu, 2010; He et al., 2017); human societies prospered relatively in these chosen destinations since ~5 ka, as inferred from the dated records of deposits in the Mu Us desert (Figs. 2 and 3) and the spatiotemporal distribution of archaeological sites (Fig. 6). In the middle and lower reaches of the Yellow River, the density of archaeological sites was substantially higher both before and after ~5–4 ka, leading to a greatly increased population and increased demand for food resources. The dominant dry-land crops (e.g., millets) and locally cultivated rice supported an enormous population (Jin et al., 2007, 2016; Zhang et al., 2010b). A similar example is the deteriorating climate during the early Bronze Age in the West Liao River Basin which forced the population to migrate southwards, to the relatively flat loess tableland that was more suitable for millet farming; and westwards to the foothills of the Greater Khingan Mountains that favored the development of animal husbandry and hunting (Jia et al., 2016). Above all, there existed cultural exchange between the Yangshao and Hongshan cultural domains (Mo et al., 2003) which facilitated

migration during the mid-Holocene.

From 5 to 4 ka, the cold and/or dry environmental conditions noted in the introduction indicate that a hemisphere-wide megadrought occurred in middle to low latitudes of the Northern Hemisphere which triggered the collapses of mid-Holocene cultures (Hsu, 1998; Weiss and Bradley, 2001). It should be noted that the indicators of cultural collapse include (1) a rapid reduction in the number of archaeological sites, (2) a reduction in the quality of the archaeological artifacts compared to the previous culture, and (3) the shift from a predominantly arable economy to pastoralism in northern China (Wu and Liu, 2004; Liu and Feng, 2012). Our conclusions suggest that the number of archaeological sites in NE China decreased during the interval from ~5 to 4 ka (Fig. 6), in accord with a low population level at ~4.5 ka inferred by a prehistoric demographic study in northern China (Wang et al., 2014b) and the distribution of archaeological sites in northern China during the late Neolithic – Bronze Age transition (Liu and Feng, 2012; Wagner et al., 2013). The absence of reaping knives and the presence of tools associated with hunting and gathering (e.g., arrowheads and grinding stones; Liu and Chen, 2012) during the Xiaoheyan cultural period suggest that pastoralism was the economic foundation with a small contribution from cultivation (Liu et al., 2016b). In addition, the disappearance of high-quality black-surface pottery in ritual burials at ~4 ka indicates that the Longshan population decreased sharply in the lower reaches of the Yellow River (Liu and Feng, 2012). Thus, our results support the view that a widespread drought destroyed the rain-fed agricultural and/or plant-based subsistence economies, ultimately contributing ultimately contributed to the collapse of the late Neolithic cultures in NE China.

6. Conclusions

Our analysis of a compilation of Holocene records of sub-aerial sedimentary deposits and lake sediments from the deserts of NE China and the adjacent regions demonstrates that the mid-Holocene environmental transition interrupted a period of relatively stable and warm climate. Our results indicate that the Holocene climate in these deserts can roughly be divided into four periods: early Holocene anathermal (~12–9 ka), Holocene Thermal Optimum (~9–6 ka), mid-Holocene environmental transition (~6–4 ka) and late Holocene deterioration (~4 ka onwards). Most likely, decreases in Northern Hemisphere summer insolation played the dominant role in weakening the EASM intensity and reducing precipitation along the margin of the EASM front, which in turn triggered the mid-Holocene environmental transition in these deserts.

During the interval from ~5 to 4 ka, the numbers of archaeological sites decreased in the study regions but they increased substantially in the middle to lower reaches of the Yellow River. An investigation of the published literature relating to late Neolithic cultures in NE China leads to the conclusion that the mid-Holocene environmental transition contributed substantially to ecosystem degradation in the deserts of NE China and the adjacent regions, which transformed land which was agriculturally productive and habitable during the Holocene Thermal Optimum to an uninhabitable state during the mid-Holocene. In response, the late Neolithic peoples likely migrated to moister and warmer regions to the south, in the middle and lower reaches of the Yellow River. Overall, a widespread mid-Holocene drought destroyed the rain-fed agricultural and/or plant-based subsistence economies, ultimately contributing to the collapse of late Neolithic cultures in NE China. If correct, this conclusion supports the speculation that one of the origins of Chinese civilization may be rooted in the adjacent regions of the deserts of NE China.

Acknowledgements

Financial support for this research was provided by the “Strategic Priority Research Program” of the Chinese Academy of Sciences (Grant XDA19050104), the National Key R&D Program of China (Grant 2017YFA0603404), the “Strategic Priority Research Program” of the Chinese Academy of Sciences (Grant XDPB0503) and the National Nature Science Foundation of China (Grant 41272206). We are grateful to Dr. Jan Bloemendal for improving an early version of the manuscript. Special thanks are extended to the editor and reviewers (Prof. Danielle Schreveth and anonymous reviewers), who expended considerable time and effort in providing valuable suggestions and critical comments on this paper.

Appendix A. Supplementary data

Supplementary data related to this article can be found at <https://doi.org/10.1016/j.quascirev.2018.04.017>.

References

- Abram, N.J., Gagan, M.K., Liu, Z., Hantoro, W.S., McCulloch, M.T., Suwargadi, B.W., 2007. Seasonal characteristics of the Indian Ocean Dipole during the Holocene epoch. *Nature* 445, 299–302.
- Abram, N.J., McGregor, H.V., Gagan, M.K., Hantoro, W.S., Suwargadi, B.W., 2009. Oscillations in the southern extent of the Indo-Pacific Warm Pool during the mid-Holocene. *Quat. Sci. Rev.* 28, 2794–2803.
- Alley, R.B., Ágústsdóttir, A.M., 2005. The 8k event: cause and consequences of a major Holocene abrupt climate change. *Quat. Sci. Rev.* 24, 1123–1149.
- Alley, R.B., Marotzke, J., Nordhaus, W.D., Overpeck, J.T., Peteet, D.M., Pielke, R.A., Pierrehumbert, R.T., Rhines, P.B., Stocker, T.F., Talley, L.D., Wallace, J.M., 2003. Abrupt climate change. *Science* 299, 2005–2010.
- Alley, R.B., Mayewski, P.A., Sowers, T., Stuiver, M., Taylor, K.C., Clark, P.U., 1997. Holocene climatic instability: a prominent, widespread event 8200 yr ago. *Geology* 25, 483–486.
- An, C.B., Feng, Z.D., Barton, L., 2006. Dry or humid? mid-Holocene humidity changes in arid and semi-arid China. *Quat. Sci. Rev.* 25, 351–361.
- An, C.B., Tang, L.Y., Barton, L., Chen, F.H., 2005. Climate change and cultural response around 4000 cal yr B.P. in the western part of Chinese Loess Plateau. *Quat. Res.* 63, 347–352.
- Bond, G., Kromer, B., Beer, J., Muscheler, R., Evans, M.N., Showers, W., Hoffmann, S., Lotti-Bond, R., Hajdas, I., Bonani, G., 2001. Persistent solar influence in North Atlantic climate during the Holocene. *Science* 294, 2130–2136.
- Bond, G., Showers, W., Cheseby, M., Lotti, R., Almasi, P., deMenocal, P., Priore, P., Cullen, H., Hajdas, I., Bonani, G., 1997. A pervasive millennial-scale cycle in the North Atlantic Holocene and glacial climates. *Science* 294, 2130–2136.
- Booth, R.K., Jackson, S.T., Forman, S.L., Kutzbach, J.E., Bettis, E.A., Kreigs, J., Wright, D.K., 2005. A severe centennial-scale drought in mid-continent North America 4200 years ago and apparent global linkages. *Holocene* 15, 321–328.
- Chen, C.T.A., Lan, H.C., Lou, J.Y., Chen, Y.C., 2003. The dry Holocene Megathermal in Inner Mongolia. *Palaeogeogr. Palaeoclimatol. Palaeoecol.* 193, 181–200.
- Chen, F.H., Dong, G.H., Zhang, D.J., Liu, X.Y., Jia, X., An, C.B., Ma, M.M., Xie, Y.W., Barton, L., Ren, X.Y., Zhao, Z.J., Wu, X.H., Jones, M.K., 2015a. Agriculture facilitated permanent human occupation of the Tibetan Plateau after 3600 B.P. *Science* 347, 248–250.
- Chen, F.H., Liu, J.B., Xu, Q.H., Li, Y.C., Chen, J.H., Wei, H.T., Liu, Q.S., Wang, Z.L., Cao, X.Y., Zhang, S.R., 2013. Environmental magnetic studies of sediment cores from Gonghai Lake: implications for monsoon evolution in North China during the late glacial and Holocene. *J. Paleolimnol.* 49, 447–464.
- Chen, F.H., Xu, Q.H., Chen, J.H., Birks, H.J.B., Liu, J.B., Zhang, S.R., Jin, L.Y., An, C.B., Telford, R.J., Cao, X.Y., Wang, Z.L., Zhang, X.J., Selvaraj, K., Lu, H.Y., Li, Y.C., Zheng, Z., Wang, H.P., Zhou, A.F., Dong, G.H., Zhang, J.W., Huang, X.Z., Bloemendal, J., Rao, Z.G., 2015b. East Asian summer monsoon precipitation variability since the last deglaciation. *Sci. Rep.* 5 (11186). <https://doi.org/10.1038/srep11186>.
- Chen, L., Shen, H.Y., Jia, Y.L., Wu, J.L., Li, X.S., Wei, L., Wang, P.L., 2008. Environmental change inferred from Rb and Sr of lacustrine sediments in Huangqihai Lake, Inner Mongolia. *J. Geogr. Sci.* 18, 373–384.
- Crawford, G.W., 2009. Agricultural origins in North China pushed back to the Pleistocene–Holocene boundary. *Proc. Natl. Acad. Sci. U. S. A* 106, 7271–7272.
- Cullen, H.M., deMenocal, P.B., Hemming, S., Hemming, G., Brown, F.H., Guilderson, F.H., Sirocko, F., 2000. Climate change and the collapse of the Akkadian empire: Evidence from the deep sea. *Geology* 28, 379–382.
- Dansgaard, W., White, J.W.C., Johnsen, S.J., 1989. The abrupt termination of the Younger Dryas climate event. *Nature* 339, 532–534.
- de Boer, E.J., Tjallingii, R., Vélez, M.I., Rijssdijk, K.F., Vlug, A., Reichart, G.-J., Prendergast, A.L., de Louw, P.G.B., Florens, F.B.V., Baider, C., Hooghiemstra, H., 2014. Climate variability in the SW Indian Ocean from an 8000-yr long multi-proxy record in the Mauritian lowlands shows a middle to late Holocene shift from negative IOD-state to ENSO-state. *Quat. Sci. Rev.* 86, 175–189.
- deMenocal, P., Ortiz, J., Guilderson, T., Adkins, J., Sarnthein, M., Baker, L., Yarusinsky, M., 2000a. Abrupt onset and termination of the Africal Humid Period: rapid climate responses to gradual insolation forcing. *Quat. Sci. Rev.* 19, 347–361.
- deMenocal, P., Ortiz, J., Guilderson, T., Sarnthein, M., 2000b. Coherent high- and low-latitude climate variability during the Holocene warm period. *Science* 288, 2198.
- deMenocal, P.B., 2001. Cultural responses to climate change during the late Holocene. *Science* 292, 667–673.
- Dodson, J.R., Li, X.Q., Zhou, X.Y., Zhao, K.L., Sun, N., Atahan, P., 2013. Origin and spread of wheat in China. *Quat. Sci. Rev.* 72, 108–111.
- Drennan, R.D., Peterson, C.E., Lu, X.M., Li, T., 2017. Hongshan households and communities in Neolithic northeastern China. *J. Anthropol. Archaeol.* 47, 50–71.
- Drysdale, R., Zanchetta, G., Hellstrom, J., Maas, R., Fallick, A., Pickett, M., Cartwright, I., Piccini, L., 2006. Late Holocene drought responsible for the collapse of Old World civilizations is recorded in an Italian cave flowstone. *Geology* 34, 101–104.
- Fan, J.W., Xiao, J.L., Wen, R.L., Zhang, S.R., Wang, X., Cui, L.L., Yamagata, H., 2017. Carbon and nitrogen signatures of sedimentary organic matter from Dali Lake in Inner Mongolia: implications for Holocene hydrological and ecological variations in the East Asian summer monsoon margin. *Quat. Int.* 452, 65–78.
- Fan, J.W., Xiao, J.L., Wen, R.L., Zhang, S.R., Wang, X., Cui, L.L., Li, H., Xue, D.S., Yamagata, H., 2016. Droughts in the East Asian summer monsoon margin during the last 6 kyrs: link to the North Atlantic cooling events. *Quat. Sci. Rev.* 151, 88–99.
- Feng, Z.D., Wang, W.G., Guo, L.L., Khosbayar, P., Narantsetseg, T., Jull, A.J.T., An, C.B., Li, X.Q., Zhang, H.C., Ma, Y.Z., 2005. Lacustrine and eolian records of Holocene climate changes in the Mongolian Plateau: preliminary results. *Quat. Int.* 136, 25–32.
- Giosan, L., Clift, P.D., Macklin, M.G., Fuller, D.Q., Constantinescu, S., Durcan, J.A., Stevens, T., Duller, G.A.T., Tabrez, A.R., Gangal, K., Adhikari, R., Alizai, A., Filip, F., VanLaningham, S., Syvitski, J.P.M., 2012. Fluvial landscapes of the Harappan civilization. *Proc. Natl. Acad. Sci. U. S. A* 109, E1688–E1694.
- Goldsmith, Y., Broecker, W.S., Xu, H., Polissar, P.J., deMenocal, P.B., Porat, N., Lan, J., Cheng, P., Zhou, W.J., An, Z., 2017a. Northward extent of East Asian monsoon covaries with intensity on orbital and millennial timescales. *Proc. Natl. Acad. Sci. U. S. A* 114, 1817–1821.
- Goldsmith, Y., Broecker, W.S., Xu, H., Polissar, P.J., deMenocal, P.B., Porat, N., Lan, J., Cheng, P., Zhou, W.J., An, Z., 2017b. Reply to Liu et al.: East Asian summer monsoon rainfall dominates Lake Dali lake area changes. *Proc. Natl. Acad. Sci. U. S. A* 114, E2989–E2990.
- Guan, Y.Y., Wang, Y., Yao, P.Y., Chi, Z.Q., Zhao, Z.L., 2010. Environmental evolution since the Holocene in the Haolaihure ancient lake, Keshiketengqi, Inner Mongolia, China. *Geol. Bull. China* 29 (6), 891–900 (In Chinese with English abstract).
- Guo, L.C., Xiong, S.F., Yang, P., Ye, W., Jin, G.Y., Wu, W.W., Zhao, H., 2018. Holocene environmental changes in the Horqin desert revealed by OSL dating and $\delta^{13}\text{C}$ analyses of paleosols. *Quat. Int.* 469, 11–19.
- Guo, L.L., Feng, Z.D., Li, X.Q., Liu, L.Y., Wang, L.X., 2007. Holocene climatic and environmental changes recorded in Baahar Nuur Lake core in the Ordos Plateau, Inner Mongolia of China. *Chin. Sci. Bull.* 52, 959–966.
- Guo, Z.T., Petit-Maire, N., Kröpelin, S., 2000. Holocene non-orbital climatic events in present-day arid areas of northern Africa and China. *Global Planet. Change* 26, 97–103.
- Haug, G.H., Hughen, K.A., Sigman, D.M., Peterson, L.C., Röhrl, U., 2001. Southward migration of the Intertropical Convergence Zone through the Holocene. *Science* 293, 1304–1308.
- He, K.Y., Lu, H.Y., Zhang, J.P., Wang, C., Huan, X.J., 2017. Prehistoric evolution of the dualistic structure mixed rice and millet farming in China. *Holocene* 27, 1885–1898.
- Hillman, A.L., Abbott, M.B., Finkenbinder, M.S., Yu, J.Q., 2017. An 8,600 year lacustrine record of summer monsoon variability from Yunnan, China. *Quat. Sci. Rev.* 174, 120–132.
- Hoff, U., Biskaborn, B.K., Dirksen, V.G., Dirksen, O., Kuhn, G., Meyer, H., Nazarova, L., Roth, A., Diekmann, B., 2015. Holocene environment of Central Kamchatka, Russia: Implications from a multi-proxy record of Two-Yurts Lake. *Global Planet. Change* 134, 101–117.
- Hosner, D., Wagner, M., Tarasov, P.E., Chen, X.C., Leipe, C., 2016. Spatiotemporal distribution patterns of archaeological sites in China during the Neolithic and Bronze Age: An overview. *Holocene* 26, 1576–1593.
- Hsu, K.J., 1998. Sun, climate, hunger, and mass migration. *Sci. China Earth Sci.* 41, 449–472.
- Huang, C.Q., Guo, L.L., 2017. Pollen evidence of a humid mid-Holocene climate from Bahar Nuur, Inner Mongolia. *Open Access Library Journal* 4 e3467. <https://doi.org/10.4236/oalib.1103467>.
- Huang, Y.P., 2003. Miaozigou yu Dabagou yizhi dongwu yihai jianding baogao. In: Wenwu Kaogu Yanjiusuo, Neimenggu (Ed.), *Miaozigou Yu Dabagou. Encyclopedia of China Publishing House*, Beijing, pp. 599–611 (In Chinese).
- Innes, J.B., Zong, Y.Q., Wang, Z.H., Chen, Z.Y., 2014. Climatic and palaeoecological changes during the mid- to late Holocene transition in eastern China: high-resolution pollen and non-pollen palynomorph analysis at Pingwang, Yangtze coastal lowlands. *Quat. Sci. Rev.* 99, 164–175.

- Jennings, A.E., Knudsen, K.L., Hald, M., Hansen, C.V., Andrews, J.T., 2002. A mid-Holocene shift in Arctic sea-ice variability on the East Greenland Shelf. *Holocene* 12, 49–58.
- Jia, X., Sun, Y.G., Wang, L., Sun, W.F., Zhao, Z.J., Lee, H.F., Huang, W.B., Wu, S.Y., Lu, H.Y., 2016. The transition of human subsistence strategies in relation to climate change during the Bronze Age in the West Liao River Basin, Northeast China. *Holocene* 26, 781–789.
- Jia, X., Yi, S.W., Sun, Y.G., Wu, S.Y., Lee, H.F., Wang, L., Lu, H.Y., 2017. Spatial and temporal variations in prehistoric human settlement and their influencing factors on the south bank of the Xar Moron River, Northeastern China. *Front. Earth Sci.* 11, 137–147.
- Jiang, W.Y., Guo, Z.T., Sun, X.J., Wu, H.B., Chu, G.Q., Yuan, B.Y., Hatté, C., Guiot, J., 2006. Reconstruction of climate and vegetation changes of Lake Bayanchagan (Inner Mongolia): Holocene variability of the East Asian monsoon. *Quat. Res.* 65, 411–420.
- Jiang, Y.J., Wang, W., Ma, Y.Z., Li, Y.Y., Liu, L.N., He, J., 2014. A preliminary study on Holocene climate change of Ordos Plateau, as inferred by sedimentary record from Bojianghaizi Lake of Inner Mongolia, China. *Quat. Sci.* 34 (3), 654–665 (In Chinese with English abstract).
- Jin, G.Y., 2004. Climate and environmental changes of the mid-Holocene epoch in North China. *Acta Archaeol. Sin.* 4, 485–505 (In Chinese with English abstract).
- Jin, G.Y., Liu, T.S., 2002. Mid-Holocene climate change in North China, and the effect on cultural development. *Chin. Sci. Bull.* 47, 408–413.
- Jin, G.Y., Wagner, M., Tarasov, P.E., Wang, F., Liu, Y.C., 2016. Archaeobotanical records of Middle and Late Neolithic agriculture from Shandong Province, East China, and a major change in regional subsistence during the Dawenkou Culture. *Holocene* 26, 1605–1615.
- Jin, G.Y., Wang, C.M., 2010. Climate and environment of the Neolithic Age in Haidai region. *J. Palaeogeogr.* 12, 355–363 (In Chinese with English abstract).
- Jin, G.Y., Yan, S.D., Udatu, T., Lan, Y.F., Wang, C.Y., Tong, P.H., 2007. Neolithic rice paddy from the Zhaojiazhuang site, Shandong, China. *Chin. Sci. Bull.* 52, 3376–3384.
- Laskar, J., Robutel, P., Joutel, F., Gastineau, M., Correia, A.C.M., Levrard, B., 2004. A long-term solution for the insolation quantities of the Earth. *Astron. Astrophys.* 428, 261–285.
- Leipe, C., Demskie, D., Tarasov, P.E., HIMPAc Project Members, 2014. A Holocene pollen record from the northwestern Himalayan lake Tso Moriri: implications for palaeoclimatic and archaeological research. *Quat. Int.* 348, 93–112.
- Li, H.W., Yang, X.P., 2016. Spatial and temporal patterns of aeolian activities in the desert belt of northern China revealed by dune chronologies. *Quat. Int.* 410, 58–68.
- Li, X.W., 2008. Development of Social Complexity in the Liaozi Area, Northeast China. Archaeopress, Oxford.
- Lillios, K.T., Blanco-González, A., Drake, B.L., López-Sáez, J.A., 2016. Mid-late Holocene climate, demography, and cultural dynamics in Iberia: A multi-proxy approach. *Quat. Sci. Rev.* 135, 138–153.
- Liu, F.G., Feng, Z.D., 2012. A dramatic climatic transition at ~4000 cal. yr BP and its cultural responses in Chinese cultural domains. *Holocene* 22, 1181–1197.
- Liu, H.Y., Xu, L.H., Cui, H.T., 2002. Holocene history of desertification along the woodland-steppe border in Northern China. *Quat. Res.* 57, 259–270.
- Liu, H.Y., Yin, Y., Zhu, J.L., Zhao, F.J., Wang, H.Y., 2010. How did the forest respond to Holocene climate drying at the forest–steppe ecotone in northern China? *Quat. Int.* 227, 46–52.
- Liu, J., Wang, Y., Wang, Y., Guan, Y.Y., Dong, J., Li, T.D., (in press). A multi-proxy record of environmental changes during the Holocene from the Haolaihure Paleolake sediments, Inner Mongolia. *Quat. Int.* <https://doi.org/10.1016/j.quaint.2016.12.015>.
- Liu, J.B., Chen, J.H., Kandasamy, S., Chen, S.Q., Xie, C.L., Chen, Q.M., Lin, B.Z., Yu, K.F., Xu, Q.H., Velasco, V.M., Chen, F.H., 2018. A 14.7 ka record of earth surface processes from the arid-monsoon transitional zone of China. *Earth Surf. Process. Landforms* 43, 723–734.
- Liu, L., Chen, X.C., 2012. The Archaeology of China: from the Late Paleolithic to the Early Bronze Age. Cambridge University Press, Cambridge, UK.
- Liu, L., Duncan, N.A., Chen, X.C., Ji, P., 2016b. Plant-based subsistence strategies and development of complex societies in Neolithic Northeast China: Evidence from grinding stones. *J. Archaeol. Sci. Rep.* 7, 247–261.
- Liu, L., Duncan, N.A., Chen, X.C., Zhao, H., Ji, P., 2016a. Changing patterns of plant-based food production during the Neolithic and Early Bronze Age in central-south Inner Mongolia, China: An interdisciplinary approach. *Quat. Int.* 419, 36–53.
- Liu, L.Y., Skidmore, E., Hasi, E., Wagner, L., Tatarko, J., 2005. Dune sand transport as influenced by wind directions, speed and frequencies in the Ordos Plateau, China. *Geomorphology* 67, 283–297.
- Liu, M.G., 2010. Atlas of Physical Geography of China, third ed. China Map Press, Beijing, p. 41 (In Chinese).
- Liu, X.Y., Jones, M.K., Zhao, Z.J., Liu, G.X., O'Connel, T.C., 2012. The earliest evidence of millet as a staple crop: new light on Neolithic foodways in north China. *Am. J. Phys. Anthropol.* 149, 283–290.
- Lu, H.Y., Mason, J.A., Stevens, T., Zhou, Y.L., Yi, S.W., Miao, X.D., 2011. Response of surface processes to climatic change in the dunefields and Loess Plateau of North China during the late Quaternary. *Earth Surf. Process. Landforms* 36, 1590–1603.
- Lu, H.Y., Miao, X.D., Zhou, Y.L., Mason, J., Swinehart, J., Zhang, J.F., Zhou, L.P., Yi, S.W., 2005. Late Quaternary aeolian activity in the Mu Us and Otindag dunefields (north China) and lagged response to insolation forcing. *Geophys. Res. Lett.* 32, L21716. <https://doi.org/10.1029/2005GL024560>.
- Lu, H.Y., Yi, S.W., Liu, Z.Y., Mason, J.A., Jiang, D.B., Cheng, J., Stevens, T., Xu, Z.W., Zhang, E.L., Jin, L.Y., Zhang, Z.H., Guo, Z.T., Wang, Y., Otto-Btiesner, B., 2013. Variation of East Asian monsoon precipitation during the past 21 k.y. and potential CO₂ forcing. *Geology* 41, 1023–1026.
- Lu, H.Y., Zhou, Y.L., Liu, W.G., Mason, J.A., 2012. Organic stable carbon isotopic composition reveals late Quaternary vegetation changes in the dunefields of northern China. *Quat. Res.* 77, 433–444.
- MacDonald, G., 2011. Potential influence of the Pacific Ocean on the Indian summer monsoon and Harappan decline. *Quat. Int.* 229, 140–148.
- Madella, M., Fuller, D.Q., 2006. Palaeoecology and the Harappan civilisation of South Asia: a reconsideration. *Quat. Sci. Rev.* 25, 1283–1301.
- Marchant, R., Hooghiemstra, H., 2004. Rapid environmental change in African and South American tropics around 4000 years before present: a review. *Earth Sci. Rev.* 66, 217–260.
- Marshall, M.H., Lamb, H.F., Huws, D., Davies, S.J., Bates, R., Bloemendal, J., Boyle, J., Leng, Melanie J., Umer, M., Bryant, C., 2011. Late Pleistocene and Holocene drought events at Lake Tana, the source of the Blue Nile. *Global Planet. Change* 78, 147–161.
- Mason, J.A., Lu, H.Y., Zhou, Y.L., Miao, X.D., Swinehart, J.B., Liu, Z.Y., Goble, R.J., Yi, S.W., 2009. Dune mobility and aridity at the desert margin of northern China at a time of peak monsoon strength. *Geology* 37, 947–950.
- Mayewski, P.A., Rohling, E.E., Stager, J.C., Karlen, W., Maasch, K.A., Meeker, L.D., Meyerson, E.A., Gasse, F., van Kreveld, S., Holmgren, K., Lee-Thorp, J., Rosqvist, G., Rack, F., Staubwasser, M., Schneider, R.R., Steig, E.J., 2004. Holocene climate variability. *Quat. Res.* 62, 243–255.
- Menzel, P., Gaye, B., Mishra, P.K., Anoop, A., Basavaiah, N., Marwan, N., Plessen, B., Prasad, S., Riedel, N., Stebich, M., Wiesner, M.G., 2014. Linking Holocene drying trends from Lonar Lake in monsoonal central India to North Atlantic cooling events. *Palaeogeogr. Palaeoclimatol. Palaeoecol.* 410, 164–178.
- Mercuri, A.M., Sadori, L., Ollero, P.U., 2011. Mediterranean and north-African cultural adaptations to mid-Holocene environmental and climatic changes. *Holocene* 21, 189–206.
- Miao, Y.F., Jin, H.L., Cui, J.X., 2016. Human activity accelerating the rapid desertification of the Mu Us Sandy Lands, North China. *Sci. Rep.* 6 (23003). <https://doi.org/10.1038/srep23003>.
- Mo, D.W., Wang, H., Li, S.C., 2003. Effects of Holocene environmental changes on the development of archaeological cultures in different regions of North China. *Quat. Sci.* 23, 200–210 (In Chinese with English abstract).
- Moros, M., Deckker, P.D., Jansen, E., Perner, K., Telford, R.J., 2009. Holocene climate variability in the Southern Ocean recorded in a deep-sea sediment core off South Australia. *Quat. Sci. Rev.* 28, 1932–1940.
- Morrill, C., Overpeck, J.T., Cole, J.E., 2003. A synthesis of abrupt changes in the Asian summer monsoon since the last deglaciation. *Holocene* 13, 465–476.
- Moy, C.M., Seltzer, G.O., Rodbell, D.T., Anderson, D.M., 2002. Variability of El Niño/Southern Oscillation activity at millennial timescales during the Holocene epoch. *Nature* 420, 162–165.
- O'Brien, S.R., Mayewski, P.A., Meeker, L.D., Meese, D.A., Twickler, M.S., Whitlow, S.I., 1995. Complexity of Holocene climate as reconstructed from a Greenland ice core. *Science* 270, 1962–1964.
- Peng, Y.J., Xiao, J.L., Nakamura, T., Liu, B.L., Inouchi, Y., 2005. Holocene East Asian monsoonal precipitation pattern revealed by grain-size distribution of core sediments of Daihai Lake in Inner Mongolia of north-central China. *Earth Planet. Sci. Lett.* 233, 467–479.
- Perry, C.A., Hsu, K.J., 2000. Geophysical, archaeological, and historical evidence support a solar-output model for climate change. *Proc. Natl. Acad. Sci. U. S. A* 97, 12433–12438.
- Peterse, F., Prins, M.A., Beets, C.J., Troelstra, S.R., Zheng, H.P., Gu, Z.Y., Schouten, S., Damsté, J.S.S., 2011. Decoupled warming and monsoon precipitation in East Asia over the last deglaciation. *Earth Planet. Sci. Lett.* 301, 256–264.
- Phillipps, R., Holdaway, S., Wendrich, W., Cappers, R., 2012. Mid-Holocene occupation of Egypt and global climatic change. *Quat. Int.* 251, 64–76.
- Ponton, C., Giosan, L., Eglington, T.I., Fuller, D.Q., Johnson, J.E., Kumar, P., Collett, T.S., 2012. Holocene aridification of India. *Geophys. Res. Lett.* 39, L03704. <https://doi.org/10.1029/2011GL050722>.
- Prasad, S., Anoop, A., Riedel, N., Sarkar, S., Menzel, P., Basavaiah, N., Krishnan, R., Fuller, D., Plessen, B., Gaye, B., Röhl, U., Wilkes, H., Sachse, D., Sawant, R., Wiesner, M.G., Stebich, M., 2014b. Prolonged monsoon droughts and links to Indo-Pacific warm pool: A Holocene record from Lonar Lake, central India. *Earth Planet. Sci. Lett.* 391, 171–182.
- Prasad, V., Farooqui, A., Sharma, A., Phartiyal, B., Chakraborty, S., Bhandari, S., Raj, R., Singh, A., 2014a. Mid-late Holocene monsoonal variations from mainland Gujarat, India: A multi-proxy study for evaluating climate culture relationship. *Palaeogeogr. Palaeoclimatol. Palaeoecol.* 397, 38–51.
- Rao, Z.G., Jia, G.D., Li, Y.X., Chen, J.H., Xu, Q.H., Chen, F.H., 2016. Asynchronous evolution of the isotopic composition and amount of precipitation in north China during the Holocene revealed by a record of compound-specific carbon and hydrogen isotopes of long-chain *n*-alkanes from an alpine lake. *Earth Planet. Sci. Lett.* 446, 68–76.
- Reimer, P.J., Bard, E., Bayliss, A., Beck, J.W., Blackwell, P.G., Bronk Ramsey, C., Buck, C.E., Cheng, H., Edwards, R.L., Friedrich, M., Grootes, P.M., Guilderson, T.P., Hajdas, I., Heaton, T.J., Hoffmann, D.L., Hogg, A.G., Hughen, K.A., Kaiser, K.F., Kromer, B., Manning, S.W., Niu, M., Reimer, R.W., Richards, D.A., Scott, E.M., Southon, J.R., Staff, R.A., Turney, C.S.M., van der Plicht, J., 2013. IntCal13 and Marine13 radiocarbon age calibration curves,

- 0–50,000 years cal BP. *Radiocarbon* 55, 1869–1877.
- Ren, M.E., Yang, R.Z., Bao, H.S., 1985. *An Outline of China's Physical Geography*. Foreign Languages Press, Beijing, pp. 346–365.
- Ren, S.N., Wu, Y.L., 1999. Zhongguo xinshiqi shidai kaoguxue wushi nian. *Near E. Archaeol.* 9, 11–22 (In Chinese).
- Roberts, N., Eastwood, W.J., Kuzucuoglu, C., Fiorentino, G., Caracuta, V., 2011. Climatic, vegetation and cultural change in the Eastern Mediterranean during the mid-Holocene environmental transition. *Holocene* 21, 147–162.
- Rudaya, N., Tarasov, P., Dorofeyuk, N., Solovieva, N., Kalugin, I., Andreev, A., Daryin, A., Diekmann, B., Riedel, F., Tserendash, N., Wagner, M., 2009. Holocene environments and climate in the Mongolian Altai reconstructed from the Hoton-Nur pollen and diatom records: a step towards better understanding climate dynamics in Central Asia. *Quat. Sci. Rev.* 28, 540–554.
- Ruddiman, W.F., Guo, Z.T., Zhou, X.Y., Wu, H.B., Yu, Y.Y., 2008. Early rice farming and anomalous methane trends. *Quat. Sci. Rev.* 27, 1291–1295.
- Russell, J., Talbot, M.R., Haskell, B.J., 2003. Mid-Holocene climate change in Lake Bosumtwi, Ghana. *Quat. Res.* 60, 133–141.
- Saraswat, R., Naik, D.K., Nigam, R., Gaur, A.S., 2016. Timing, cause and consequences of mid-Holocene climate transition in the Arabian Sea. *Quat. Res.* 86, 162–169.
- Sarkar, S., Prasad, S., Wilkes, H., Riedel, N., Stebich, M., Basavaiah, N., Sachse, D., 2015. Monsoon source shifts during the drying mid-Holocene: biomarker isotope based evidence from the core 'monsoon zone' (CMZ) of India. *Quat. Sci. Rev.* 123, 144–157.
- Schettler, G., Liu, Q., Mingram, J., Stebich, M., Dulski, P., 2006. East-Asian monsoon variability between 15000 and 2000 cal. yr BP recorded in varved sediments of Lake Sihaolongwan (northeastern China, Long Gang volcanic field). *Holocene* 16, 1043–1057.
- Scussolini, P., Vegas-Vilarrubia, T., Rull, V., Corella, J.P., Valero-Garcés, B., Gomà, J., 2011. Middle and late Holocene climate change and human impact inferred from diatoms, algae and aquatic macrophyte pollen in sediments from Lake Montcortès (Ne Iberian Peninsula). *J. Paleolimnol.* 46, 369–385.
- Shanahan, T.M., McKay, N.P., Hughen, K.A., Overpeck, J.T., Ottobiesner, B., Heil, C.W., King, J., Scholz, C.A., Peck, J., 2015. The time-transgressive termination of the African Humid Period. *Nat. Geosci.* 8, 140–144.
- Shen, H.Y., Jia, Y.L., Guo, F., 2010. Characteristics and environmental significance of the magnetic susceptibility in sediment of Huangqihai Lake, Inner Mongolia. *China. Arid Land Geogr.* 33, 151–157 (In Chinese with English abstract).
- Shen, H.Y., Zhang, H.M., Jia, Y.L., 2005. An organic carbon isotopic record from sediments of the Huangqihai Lake, Inner Mongolia: implications of environmental evolution. *Mar. Geol. Quat. Geol.* 25, 35–40 (In Chinese with English abstract).
- Shi, P.J., Song, C.Q., 2003. Palynological records of environmental changes in the middle part of Inner Mongolia, China. *Chin. Sci. Bull.* 48, 1433–1438.
- Singhvi, A.K., Bluszcz, A., Bateman, M.D., Rao, M.S., 2001. Luminescence dating of loess-paleosol sequences and coversands: methodological aspects and palaeoclimatic implications. *Earth Sci. Rev.* 54, 193–211.
- Solomina, O.N., Bradley, R.S., Hodgson, D.A., Ivy-Ochs, S., Jomelli, V., Mackintosh, A.N., Nesje, A., Owen, L.A., Wanner, H., Wiles, G.C., Young, N.E., 2015. Holocene glacier fluctuations. *Quat. Sci. Rev.* 111, 9–34.
- Staubwasser, M., Sirocko, F., Grootes, P.M., Segl, M., 2003. Climate change at the 4.2 ka BP termination of the Indus Valley civilization and Holocene south Asian monsoon variability. *Geophys. Res. Lett.* 30, 1425. <http://dx.doi.org/10.1029/2002GL016822>.
- Stott, L., Cannariato, K., Thunell, R., Haug, G.H., Koutavas, A., Lund, S., 2004. Decline of surface temperature and salinity in the western tropical Pacific Ocean in the Holocene epoch. *Nature* 431, 56–59.
- Stuiver, M., Reimer, P.J., 1993. Extended ^{14}C data base and revised CALIB 3.0 ^{14}C age calibration program. *Radiocarbon* 35, 215–230.
- Sun, A.Z., Feng, Z.D., 2013. Holocene climatic reconstructions from the fossil pollen record at Qigai Nuur in the southern Mongolian Plateau. *Holocene* 23, 1391–1402.
- Tang, L., Wang, X.S., Zhang, S.Q., Chu, G.Q., Yun, C., Pei, J.L., Sheng, M., Yang, Z.Y., 2015. High-resolution magnetic and palynological records of the last deglaciation and Holocene from Lake Xiarinur in the Hunshandake Sandy Land, Inner Mongolia. *Holocene* 25, 844–856.
- Tarasov, P.E., Jin, G.Y., Wagner, M., 2006. Mid-Holocene environmental and human dynamics in northeastern China reconstructed from pollen and archaeological data. *Palaeogeogr. Palaeoclimatol. Palaeoecol.* 241, 284–300.
- Thompson, L.G., Mosley-Thompson, E., Davis, M.E., Henderson, K.A., Brecher, H.H., Zagorodnov, V.S., Mashioita, T.A., Lin, P.-N., Mikhalenko, V.N., Hardy, D.R., Beer, J., 2002. Kilimanjaro ice core records: evidence of Holocene climate change in tropical Africa. *Science* 298, 589–593.
- Wagner, M., Tarasov, P., Hosner, D., Fleck, A., Ehrlich, R., Chen, X.C., Leipe, C., 2013. Mapping of the spatial and temporal distribution of archaeological sites of northern China during the Neolithic and Bronze Age. *Quat. Int.* 290–291, 344–357.
- Wang, H.P., Chen, J.H., Zhang, X.J., Chen, F.H., 2014a. Palaeosol development in the Chinese Loess Plateau as an indicator of the strength of the East Asian summer monsoon: Evidence for a mid-Holocene maximum. *Quat. Int.* 334, 155–164.
- Wang, F.Y., Song, C.Q., Sun, X.J., 1999. Palynological record of paleovegetation change during Holocene at north Tund Plain in Inner Mongolia, China. *Chin. Geogr. Sci.* 9, 87–91.
- Wang, C., Lu, H.Y., Zhang, J.P., Gu, Z.Y., He, K.Y., 2014b. Prehistoric demographic fluctuations in China inferred from radiocarbon data and their linkage with climate change over the past 50,000 years. *Quat. Sci. Rev.* 98, 45–59.
- Wang, H.Y., Liu, H.Y., Cui, H.T., Abrahamsen, N., 2001. Terminal Pleistocene/Holocene palaeoenvironmental changes revealed by mineral-magnetism measurements of lake sediments for Dali Nor area, southeastern Inner Mongolia Plateau, China. *Palaeogeogr. Palaeoclimatol. Palaeoecol.* 170, 115–132.
- Wang, H.Y., Liu, H.Y., Liu, Y.H., Cui, H.T., 2004. Mineral magnetism of lacustrine sediments and Holocene palaeoenvironmental changes in Dali Nor area, southeast Inner Mongolia Plateau, China. *Palaeogeogr. Palaeoclimatol. Palaeoecol.* 208, 175–193.
- Wang, H.Y., Liu, H.Y., Zhao, F.J., Yin, L., Zhu, J.L., Snowball, I., 2012a. Early- and mid-Holocene palaeoenvironments as revealed by mineral magnetic, geochemical and palynological data of sediments from Bai Nuur and Ulan Nuur, southeastern Inner Mongolia Plateau, China. *Quat. Int.* 250, 100–118.
- Wang, H.Y., Liu, H.Y., Zhu, J.L., Yin, Y., 2010. Holocene environmental changes as recorded by mineral magnetism of sediments from Anguli-nuur Lake, southeastern Inner Mongolia Plateau, China. *Palaeogeogr. Palaeoclimatol. Palaeoecol.* 285, 30–49.
- Wang, L., Li, J.J., Lu, H.Y., Gu, Z.Y., Rioual, P., Hao, Q.Z., Mackay, A.M., Jiang, W.Y., Cai, B.G., Xu, B., Han, J.T., Chu, G.Q., 2012b. The East Asian winter monsoon over the last 15,000 years: its links to high-latitudes and tropical climate systems and complex correlation to the summer monsoon. *Quat. Sci. Rev.* 32, 131–142.
- Wang, W., Feng, Z.D., 2013. Holocene moisture evolution across the Mongolian Plateau and its surrounding areas: A synthesis of climatic records. *Earth Sci. Rev.* 122, 38–57.
- Wanner, H., Beer, J., Bütkofer, J., Crowley, T.J., Cubasch, U., Flückiger, J., Goosse, H., Grosjean, M., Joos, F., Kaplan, J.O., Küttel, M., Müller, S., Prentice, I.C., Solomina, O., Stocker, T.F., Tarasov, P., Wagner, M., Widmann, M., 2008. Mid- to Late Holocene climate change: an overview. *Quat. Sci. Rev.* 27, 1791–1828.
- Wanner, H., Solomina, O., Grosjean, M., Ritz, S.P., Jetel, M., 2011. Structure and origin of Holocene cold events. *Quat. Sci. Rev.* 30, 3109–3123.
- Weiss, H., Bradley, R.S., 2001. What drives societal collapse? *Science* 291, 609–610.
- Weiss, H., Courtney, M.-A., Wetterstrom, W., Guichard, F., Senior, L., Meadow, R., Curnow, A., 1993. The genesis and collapse of third millennium north Mesopotamian civilization. *Science* 261, 995–1004.
- Wen, R.L., Xiao, J.L., Chang, Z.G., Zhai, D.Y., Xu, Q.H., Li, Y.C., Itoh, S., Lomtatidze, Z., 2010. Holocene climate changes in the mid-high latitude monsoon margin reflected by the pollen record from Hulun Lake, northeastern Inner Mongolia. *Quat. Res.* 73, 293–303.
- Wen, R.L., Xiao, J.L., Fan, J.W., Zhang, S.R., Yamagata, H., 2017. Pollen evidence for a mid-Holocene East Asian summer monsoon maximum in northern China. *Quat. Sci. Rev.* 176, 29–35.
- Wu, W.X., Liu, T.S., 2004. Possible role of the "Holocene event 3" on the collapse of Neolithic Cultures around the Central Plain of China. *Quat. Int.* 117, 153–166.
- Xiao, J.L., Chang, Z.G., Si, B., Qin, X.G., Itoh, S., Lomtatidze, Z., 2009b. Partitioning of the grainsize components of Dali Lake core sediments: evidence for lake-level changes during the Holocene. *J. Paleolimnol.* 42, 249–260.
- Xiao, J.L., Chang, Z.G., Wen, R.L., Zhai, D.Y., Itoh, S., Lomtatidze, Z., 2009a. Holocene weak monsoon intervals indicated by low lake levels at Hulun Lake in the monsoonal margin region of northeastern Inner Mongolia, China. *Holocene* 19, 899–908.
- Xiao, J.L., Si, B., Zhai, D.Y., Itoh, S., Lomtatidze, Z., 2008. Hydrology of Dali Lake in central-eastern Inner Mongolia and Holocene East Asian monsoon variability. *J. Paleolimnol.* 40, 519–528.
- Xiao, J.L., Wu, J.T., Si, B., Liang, W.D., Nakamura, T., Liu, B.L., Inouchi, Y., 2006. Holocene climate changes in the monsoon/arid transition reflected by carbon concentration in Daihai Lake of Inner Mongolia. *Holocene* 16, 551–560.
- Xiao, J.L., Xu, Q.H., Nakamura, T., Yang, X.L., Liang, W.D., Inouchi, Y., 2004. Holocene vegetation variation in the Daihai Lake region of north-central China: a direct indication of the Asian monsoon climatic history. *Quat. Sci. Rev.* 23, 1669–1679.
- Xu, Q.H., Xiao, J.L., Li, Y.C., Tian, F., Nakagawa, T., 2010. Pollen-based quantitative reconstruction of Holocene climate changes in the Daihai Lake area, Inner Mongolia, China. *J. Clim.* 23 (11), 2856–2868.
- Yang, X.P., Li, H.W., Conacher, A., 2012. Large-scale controls on the development of sand seas in northern China. *Quat. Int.* 250, 74–83.
- Yang, X.P., Scuderi, L., Paillou, P., Liu, Z.T., Li, H.W., Ren, X.Z., 2011. Quaternary environmental changes in the drylands of China – A critical review. *Quat. Sci. Rev.* 30, 3219–3233.
- Yang, X.P., Scuderi, L.A., Wang, X.L., Scuderi, L.J., Zhang, D.G., Li, H.W., Forman, S., Xu, Q.H., Wang, R.C., Huang, W.W., Yang, S.X., 2015. Groundwater sapping as the cause of irreversible desertification of Hunshandake Sandy Lands, Inner Mongolia, northern China. *Proc. Natl. Acad. Sci. U. S. A.* 112, 702–706.
- Yang, X.P., Wang, X.L., Liu, Z.T., Li, H.W., Ren, X.Z., Zhang, D.G., Ma, Z.B., Rioual, P., Jin, X.D., Scuderi, L., 2013. Initiation and variation of the dunefields in semi-arid northern China – with a special reference to the Hunshandake Sandy Land, Inner Mongolia. *Quat. Sci. Rev.* 78, 369–380.
- Yin, Y., Liu, H.Y., He, S.Y., Zhao, F.J., Zhu, J.L., Wang, H.Y., Liu, G., Wang, X.C., 2011. Patterns of local and regional grain size distribution and their application to Holocene climate reconstruction in semi-arid Inner Mongolia, China. *Palaeogeogr. Palaeoclimatol. Palaeoecol.* 307, 168–176.
- Zeng, M.X., Ma, C.M., Zhu, C., Song, Y.G., Zhu, T.X., He, K.Y., Chen, J., Huang, M., Jia, T.J., Guo, T.H., 2016. Influence of climate change on the evolution of ancient culture from 4500 to 3700 cal. yr BP in the Chengdu Plain, upper reaches of the Yangtze River, China. *Catena* 147, 742–754.
- Zhai, D.Y., Xiao, J.L., Zhou, L., Wen, R.L., Chang, Z.G., Wang, X., Jin, X.D., Pang, Q.Q., Itoh, S., 2011. Holocene East Asian monsoon variation inferred from species assemblage and shell chemistry of the ostracodes from Hulun Lake, Inner

- Mongolia. *Quat. Res.* 75, 512–522.
- Zhang, Q.C., Eng, J.T., Wei, J., Zhu, H., 2010b. Paleodietary studies using stable carbon and nitrogen isotopes from human bone: an example from the Miaozigou site, Qahar Youyi Qianqi, Inner Mongolia. *Acta Anthropol. Sin.* 29, 270–275 (In Chinese with English abstract).
- Zhang, J.P., Lu, H.Y., Wu, N.Q., Li, F.J., Yang, X.Y., Wang, W.L., Ma, M.Z., Zhang, X.H., 2010b. Phytolith evidence for rice cultivation and spread in Mid-Late Neolithic archaeological sites in central North China. *Boreas* 39, 592–602.
- Zhang, X.L., Wang, J.X., Xian, Z.Q., Qiu, S.H., 2003. Studies on ancient human diet. *Near E. Archaeol.* 425, 62–75 (In Chinese with English abstract).
- Zhao, Y., Yu, Z.C., 2012. Vegetation response to Holocene climate change in East Asian monsoon-margin region. *Earth Sci. Rev.* 113, 1–10.
- Zhao, Y., Yu, Z.C., Chen, F.H., Zhang, J.W., Yang, B., 2009. Vegetation response to Holocene climate change in monsoon-influenced region of China. *Earth Sci. Rev.* 97, 242–256.
- Zhao, Z.J., 2011. New archaeobotanic data for the study of the origins of agriculture in China. *Curr. Anthropol.* 52, S295–S306.
- Zhao, Z.J., 2004. Cong Xinglonggou yizhi fuxuan jieguo tan Zhongguo beifang zaoqi nongye qiyuan wenti (Addressing the origins of agriculture in north China based on the results of flotation from the Xinglonggou site). In: Guwu, Dongya (Ed.), Department of Archaeology and Museum. Nanjing Normal University. Wenwu Press, Beijing, pp. 188–199 (In Chinese).
- Zhu, X.H., Li, B., Ma, C.M., Zhu, C., Wu, L., Liu, H., 2017. Late Neolithic phytolith and charcoal records of human activities and vegetation change in Shijiahe culture, Tanjialing site, China. *PLoS One* 12 e0177287. <https://doi.org/10.1371/journal.pone.0177287>.